




The formation of nitric acid inside a BWR containment after severe accident

Authors: Niina Könönen, Jukka Rossi, Karri Penttilä

Confidentiality: Public

Report's title		
The formation of nitric acid inside a BWR containment after severe accident		
Customer, contact person, address	Order reference	
SAFIR2014 Research Program	24/2011SAF	
Project name	Project number/Short name	
Chemistry of fission products (FISKE)	73760/ FISKE2011/Safir2014	
Author(s)	Pages	
Niina Könönen, Jukka Rossi, Karri Penttilä	39	
Keywords	Report identification code	
Severe accident, nitric acid, irradiation	VTT-R-01408-12	
Summary		
<p>In this study the formation of nitric acid is estimated inside a NPP containment after severe accident using Olkiluoto 1 and 2 BWR as an example plant. Firstly, a main steam line break accident progression and some boundary conditions were calculated with the MELCOR 1.8.6 code. Secondly, radioactivity and doses of the most significant radioisotopes in the containment gas phase and water pools were calculated. Nuclide specific radioactivities were obtained by the ORIGEN2 code. Finally, the pHs of water pools were calculated using a new developed ChemPool program.</p> <p>The formation of nitric acid in pedestal pool was 5.6 kg and in wetwell pool 8.7 kg. In water pool of pedestal most of the acid is coming from cables in form of HCl, 117.5 kg. Due this the pH drops rapidly to 2. The influence of nitric acid is small about 5 %. Also in wetwell the formation of nitric acid is small and the pH of wetwell pool stays alkaline due to CsOH. In these results only the formation of nitric acid in water phases were calculated. This formation is very small and it is calculated that the dissolved nitrogen in water phase will be enough and do not limit this reaction.</p>		
Confidentiality	Public	
Espoo 22.2.2012		
Written by	Reviewed by	Accepted by
		
Niina Könönen, Research Scientist	Tommi Kekki, Senior Scientist	Timo Vanttola, Technology Manager
VTT's contact address		
PO Box 1000, 02044 VTT, Finland		
Distribution (customer and VTT)		
SAFIR2014 Reference group 5		
VTT: Timo Vanttola, Eija Karita Puska		
<p><i>The use of the name of the VTT Technical Research Centre of Finland (VTT) in advertising or publication in part of this report is only permissible with written authorisation from the VTT Technical Research Centre of Finland.</i></p>		

Contents

1	Introduction.....	3
2	Methods.....	3
2.1	MELCOR.....	4
2.2	Dose calculation models.....	4
2.2.1	Dose in the air volume	5
2.2.2	Dose in the water volume.....	6
2.2.3	Dose to pool from the core debris	7
2.3	ChemPool	7
3	Results	11
3.1	MELCOR results	11
3.1.1	Time scale.....	11
3.1.2	Temperatures and pressures	12
3.1.3	Masses.....	15
3.1.4	Radioactive releases.....	17
3.2	Dose results	27
3.2.1	Doses in the gas phase.....	27
3.2.2	Doses in the water pools.....	31
3.3	Chempool results	34
4	Conclusions and Summary.....	38
	References	39

1 Introduction

Nitric acid (HNO_3) is produced by the irradiation of water and air. The mechanism for nitric acid is not well known. Nitric acid formation with irradiation has previously been studied in ORNL by Beahm et al, (1992) NUREG/CR-5950. The radiation G value (molecules/100 eV) for nitric acid formation based radiation absorption by water was $G(\text{HNO}_3) = 0.007$ molecules/100 eV [Beahm et al. 1992]. However, very little further studies have been performed although NUREG/CR-5950 formulas are applied in plant evaluation and pool pH estimation.

2 Methods

In this study the formation of nitric acid is estimated inside a NPP containment after severe accident using Olkiluoto 1 and 2 BWR as an example plant (Figure 1). Firstly, the selected severe accident progression and some boundary conditions were calculated with the MELCOR 1.8.6 code. Secondly, radioactivity and doses of the most significant radioisotopes in the containment gas phase and water pools were calculated using ORIGEN2 code. Finally, the pHs of water pools were calculated using a new developed ChemPool program.

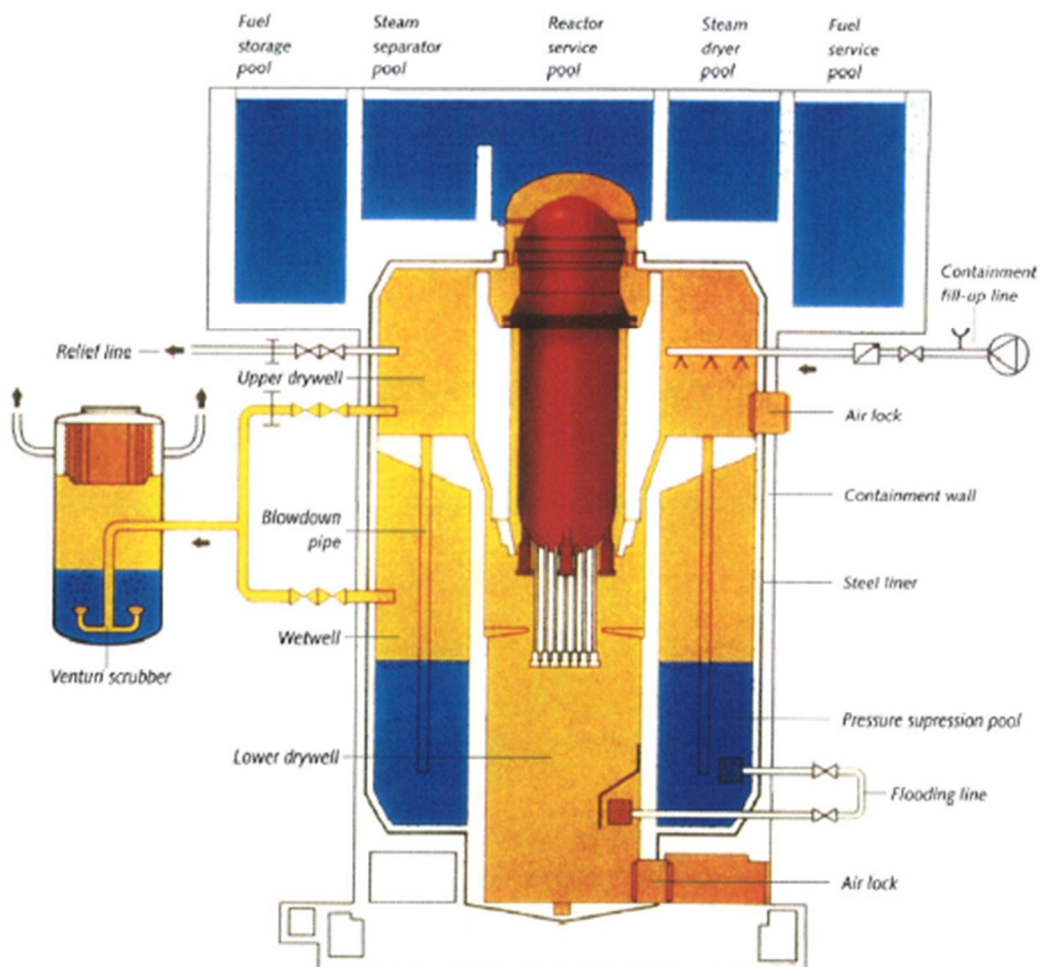


Figure 1. Olkiluoto 1 and 2 – Containment system

2.1 MELCOR

The investigated accident scenario was a basic LOCA scenario with a break in the main steam line. The steam line break was already modelled in the MELGEN input and was only activated for this simulation. According to the input the steam line breaks at 0.0 seconds. At the beginning the area of the flow path is 30 m², but in time the area gets smaller and becomes 0 m² at 0.2 seconds.

The second major change was adding the needed plot commands to the input file. The radioactive releases were studied inside the containment volumes (wetwell, drywell, biological shield and the pedestal) and in the environment. Noble gases, caesium, caesium iodide and tellurium releases were studied as aerosols in gas and in liquid as well as deposited masses on containment volume surfaces (floors and walls). Usually plot commands do not include tellurium releases, however, in this study they were added for more precise calculations.

The third change was adding the EDF commands at the end of the input file. The results of MELCOR calculations are used in a program called ChemPool developed by Karri Penttilä from VTT. CHEMPOOL program uses information on the radioactive releases, flow paths and masses which MELCOR defines. This required information is sent to an external data file (EDF) by adding EDF plot commands to the end of the input. As a result MELGEN prints out two EDF – files, which include all the required data.

The results were analysed using the PTFREAD 1.77 program developed also at the Sandia National Laboratories. The biggest interests in analysing the results were the radioactive releases. Here the results have been presented for noble gases, cesium, cesium iodide and tellurium. Iodine has not been discussed in this report, since it does not occur in the reactor as iodine but only as cesium iodide. Despite their names, different radioactive release groups may actually contain more than one element. The correct compositions of different groups are:

Noble gases: Kr, Xe
Cesium: Rb, Cs
Cesium iodide: CsI
Tellurium: Te

This means, that the group of Cesium also includes Rb releases. The original masses of each element are input to MELGEN and this information was also needed in the later analyses.

2.2 Dose calculation models

This part of the study is aimed at assessing radiation doses in the containment of the Olkiluoto BWR reactor as a consequence of the main steam line break. This accident results in core melt and a significant fraction of the radioactive material is released to the containment. Input data for radiation dosage calculations was obtained by the MELCOR calculation, in which spreading of the radioactive material in different volumes of the containment was determined. Accident sequence was followed until core debris melted a hole in the reactor cavity.

Radiation dose estimates in the water are needed for estimation of nitric acid production.

Because there is radioactive material in air, in water, on the surfaces and in the core debris, different methods are needed to obtain radiation dosage in the ambient volume. However, contribution from the air space to water and vice versa are ignored in this work.

MELCOR calculates the masses of the elementary classes combining radionuclides with similar chemical character as a function of time in the containment. On the other hand the results of the ORIGEN2 code [ORIGEN 1991] include both masses and radioactivities for all isotopes of the Olkiluoto BWR reactor inventory as a function of time. Based on the ORIGEN2 nuclide distribution, the mass of the MELCOR class can be divided into isotope masses. Thus combining these two input data isotope specific radioactive inventory for a MELCOR result can be obtained as a function of time in the containment.

MELCOR calculates also masses deposited on the surfaces. To simplify calculations the deposited mass is added to the mass in the air volume of the same room.

2.2.1 Dose in the air volume

Beta dose in the room air volume is calculated using “Infinite Cloud” assumptions, i.e., the dimensions of the contaminated air are assumed to be large compared to the distances that the beta particles travel [NRC 1972]. For an infinite uniform cloud, the beta dose rate in air is:

$$D_{\beta,i} = 0.457 \cdot X_i \cdot E_{\beta,i}, \quad (1)$$

where:

$D_{\beta,i}$ = Beta dose rate from an infinite cloud, nuclide i (rad/s),
 X_i = Concentration of beta emitting isotope i in the room air volume (curie/m³),
 $E_{\beta,i}$ = Average beta energy of nuclide i per disintegration (MeV/dis).

For gamma emitting material the dose rate in the room air volume is [NRC 1972]:

$$D_{\gamma,i} = 0.507 \cdot X_i \cdot E_{\gamma,i} \cdot (1/G), \quad (2)$$

where:

$D_{\gamma,i}$ = Gamma dose rate from an infinite cloud, nuclide i (rad/s),
 X_i = Concentration of gamma emitting isotope i in the room air volume (curie/m³),
 $E_{\gamma,i}$ = Average gamma energy of nuclide i per disintegration (MeV/dis),
 G = Geometry correction factor.

The geometry correction factor addresses the fact that the containment room atmosphere is a limited volume and it is thus inappropriately conservative to assume an infinite cloud of activity. The geometry correction factor is the ratio of

the effective dose from an infinite cloud of activity to the effective dose from a finite cloud of activity and is calculated as [Murphy et al 1974]:

$$G = 351.6/V^{0.338}, \quad (3)$$

where:

V = room volume (m^3).

The averaged beta and gamma energies can be found in [Eckerman et al 1993].

2.2.2 Dose in the water volume

Assuming that radioactive material is uniformly distributed in the water pool both beta and gamma radiation dosage in the ambient water can be obtained. Beta particles have mean free paths less than 1 cm, therefore it can be concluded that all beta energy is absorbed in water. In the case of gamma radiation due to longer travel significant energy may escape absorption by water. Absorbed doses to water pools in severe accident sequences have been studied in [Weber 1991]. The average energy absorbed in water from γ decay is

$$E_\gamma = A + B\left(\frac{S}{V}\right), \quad (4)$$

where

E_γ = average energy (MeV),

A = nuclide specific constant,

B = nuclide specific constant,

S = surface area (m^2),

V = volume (m^3).

A correlation was developed linking absorbed dose to source energy and surface-to-volume ratio of the pool. Several rectangular pools were studied. These results are now assumed to be transferable to pools of any geometry meaning that the only geometrical factor affecting energy absorption is the surface-to-volume ratio. Absorbed dose per unit mass of nuclide from beta and gamma radiation to water pool is calculated as:

$$d = 1.602 \cdot 10^{-11} \frac{(E_\beta + E_\gamma)\lambda N_a}{Mm_{wat}}, \quad (5)$$

where

d = specific dose rate due to electrons and photons (rad/s-g),

E_β = average energy (MeV) absorbed in water per β decay,

E_γ = average energy (MeV) absorbed in water per γ decay,

λ = nuclide decay constant (s^{-1}),

N_a = Avogadro's number,

M = atomic weight of nuclide,

m_{wat} = mass of water present (kg).

2.2.3 Dose to pool from the core debris

After RPV bottom failure the core melt is transferred to the water pool in the pedestal. The radioactive material in the core debris causes radiation to the ambient water. Dose calculations in this case are carried out by the MARMER code [Kloosterman 1990].

MARMER is a point-kernel shielding code. It makes use of a Monte-Carlo integration technique to perform the integration over energy range and source volume. MARMER is validated with experiments and other shielding codes.

For calculation it is assumed that the core debris is uniformly distributed on the bottom of the pedestal. The core debris forms a cylinder with the radius of 4.5 m and the height of 16.5 cm. Above this source there is a 10 meter high water cylinder in which radiation energy is absorbed.

2.3 ChemPool

Currently MELCOR code is not able to consider aqueous species and how they affect the pH in the pools. In earlier projects in VTT ChemSheet® [Hack et al 1999] was coupled with MELCOR to calculate the equilibrium composition and the pH values of the pools. After MELCOR simulation the results from MELCOR are exported to text files containing temperatures, pressures and compositions of the pools at each time steps. The estimated formation rates of acids and dissolved salts from fission products are then coupled with these and the equilibrium compositions and the pH values of the pools are calculated with ChemSheet in Excel. Internally ChemSheet uses thermodynamic programming library, ChemApp®, for calculating the equilibrium composition of a thermodynamic system (gas, water pool and solids like fission products) by minimizing its Gibbs energy.

The problem with ChemSheet model was that it needed to be tailored by hand for each MELCOR case and chemistry model separately which was time consuming process and susceptible to making errors. More advanced and properly validated software is required. Coupling of MELCOR data with thermodynamic calculation should be automated in code as much as possible. So a new simulation software, ChemPool, was made. It is a Command Prompt program (it lacks user interface) using again ChemApp thermodynamic library for equilibrium calculation.

ChemPool reads the same input file as MELCOR for setting the flowsheet (network of pools). It also modifies MELCOR input file by adding (when requested to do so) the required definitions so that MELCOR will generate a result file containing the temperatures and the compositions of the pools and the flow rates of those components between the pools (external datafile records). ChemPool uses this file to setup the pool conditions at each time step. Then user needs only to add time dependent formation rates and pool locations of those species that are not handled by MELCOR to a separate ChemPool input file so that they are added to the pH calculation, i.e. species like HNO₃ and/or HCl that are formed in pools and/or pool atmosphere due to irradiation.

Figure 2 shows a simple network of pools and Figure 3 shows the simulation algorithm.

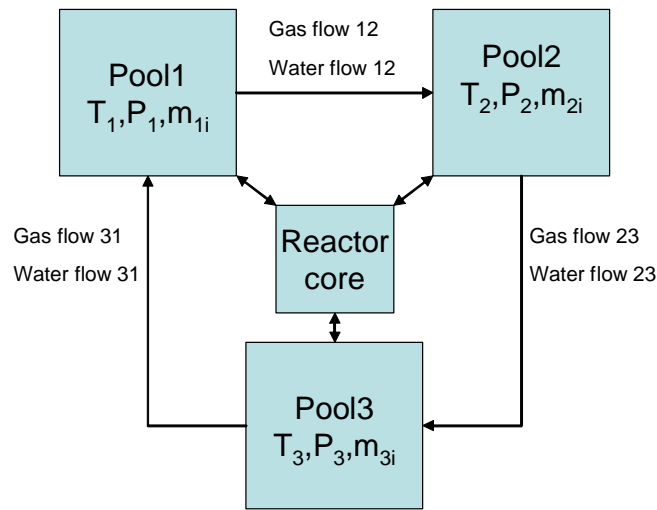


Figure 2. Example layout of a simple pool system

So temperature, T , pressure, P , and masses, m_i , of materials and classes (i.e. species) at different time steps are read from the external datafile generated by MELCOR. Then species like HNO_3 and HCl can be added to those pools after which their equilibrium compositions and pH values are calculated. And now that MELCOR also calculates the flow rates between the pools, ChemPool is also able use that information in order to calculate how these additional species flow between the pools by assuming that the pools are ideally stirred tanks, i.e. concentrations of species in pool are uniform (simplifying assumption).

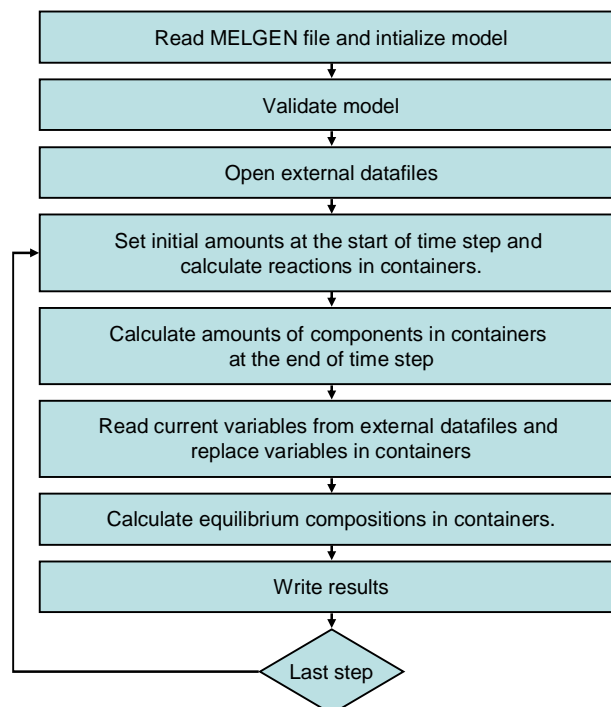


Figure 3. Simulation algorithm

In MELCOR the chemical species are defined as Materials (like water vapour (H₂O(g)), water (H₂O(a)), nitrogen gas (N₂(g)), ..) and Classes (like fission products CsI(s) and CsOH(s)). These same species are also found from the thermodynamic system used by ChemPool. Table 1 shows how the species are mapped from MELCOR to ChemPool.

Table 1. Mapping of MELCOR Materials and Classes to ChemPool species.

Type	Name/ID	Chemapp name	Description
Material	POOL	H2O/H2O	MELCOR default material - water in pool
Material	FOG	H2O/H2O	MELCOR default material - water in gas as fog
Material	H2O-VAP	Gas/H2O(g)	MELCOR default material - water vapor
Material	N2	Gas/N2(g)	MELCOR optional material
Material	O2	Gas/O2(g)	MELCOR optional material
Material	H2	Gas/H2(g)	MELCOR optional material
Material	CO	Gas/CO(g)	MELCOR optional material
Material	CO2	Gas/CO2(g)	MELCOR optional material
Material	CH4	Gas/CH4(g)	MELCOR optional material
CLASS		2 CsOH	MELCOR default class
CLASS		16 CsI	MELCOR default class
CLASS	CH3I	CH3I	iodine pool model class
CLASS	HCL	HCl	iodine pool model class
CLASS	HNO3	HNO3	iodine pool model class
CLASS	IM	-	iodine pool model class
CLASS	HBO2	H3BO3	iodine pool model class
CLASS	HPO4	Na3PO4	iodine pool model class
CLASS	LIBO	-	
REACTION		Any Chemapp species	ChemPool source term

Table 2 shows the thermodynamic system that has been used in the pH calculations. It contains a gas phase that uses Tsonopoulos model for non-ideal gas (for high pressure conditions), an aqueous water phase that uses Pitzer electrolyte model, and pure solid phases that are mainly used to input various acidic and basic salts and oxides into pools.

Table 2. Thermodynamic system

Phase	Constituent	Element												
		B	C	Cl	Cs	H	I	N	Na	O	P	e-	H2O	HNO3
Gas	H2O(g)					2				2			1	
	N2(g)							2						
	O2(g)									2				
	H2(g)					2								
	CO(g)		1								1			
	CO2(g)		1							2				
	CH4(g)		1			4								
	HI(g)					1	1							
	I2(g)						2							
	HCl(g)			1		1								
	HNO3(g)					1		1		3				1
	CsI(g)				1		1							
	CsOH(g)				1	1					1			
	H3BO3(g)	1				3					3			
Water	H2O(a)					2				1				
	B(OH)3(a)	1				3				3				
	B(OH)4(-a)	1				4				4				
	Cl(-a)			1								1		
	Cs(+a)				1							-1		
	CsOH(a)				1	1				1				
	H(+a)					1						-1		
	I(-a)						1					1		
	I2(a)						2							
	Na(+a)								1			-1		
	OH(-a)					1				1		1		
	N2(a)							2						
	HNO3(a)					1	1			3			1	
	NH3(a)					3		1						
	NH4(+a)					4		1				-1		
	NO2(-a)						1			2		1	1	
	NO3(-a)							1		3		1	1	
	H2PO4(-a)					2				4	1	1		
	HPO4(-2a)					1				4	1	2		
	PO4(-3a)									4	1	3		
	H3PO4(a)					3				4	1			
	CO2(a)		1							2				
	CO3(-2a)		1							3		2		
	HCO2(-a)		1			1				2		1		
	HCO3(-a)		1			1				3		1		
	NaCO3(-a)		1						1	1	3	1		
	Solids	CsI(s)				1		1						
CsOH(s)					1	1				1				
H3BO3(s)		1				3				3				
Na2O*2B2O3*10H2O(s)		2				20			2	17				
Na2O*5B2O3*10H2O(s)		5				20			2	26				
NaCl(s)				1				1	1					
NaOH(s)						1		1	1	1				
Na3PO4(s)								3	3	4	1			
Na2HPO4(s)						1		2	2	4	1			
NaH2PO4(s)						2		1	1	4	1			
HCl(s)				1		1								
HNO3(s)						1			1	3				
Constraints		H2O(g)+											1	
	H2O(g)-											-1		

Species have been selected from HSC® and FactSage® databases. Aqueous phase Pitzer interaction parameters were taken from VTT's in-house database and its data has been collected from various literature sources. Thermodynamic data has been validated with a separate ChemSheet model that uses the same thermodynamic system in its calculations. In this model the pH values at different temperatures and compositions are calculated and verified against measured pH values (that have been collected from literature).

3 Results

3.1 MELCOR results

3.1.1 Time scale

Table 3 presents the accident progression and the time scales of the most important events.

Table 3. Time scale of the accident scenario

Time(s)	Time (h)	Event
0.00	0 h 0 min	Reactor scram
0.00	0 h 0 min	Time of core uncover
1010.30	0 h 17 min	Zr oxidation begins
1063.30	0 h 18 min	Gap release in rod group 2
1064.80	0 h 18 min	Gap release in rod group 1
1088.30	0 h 18 min	Gap release in rod group 3
1272.21	0 h 21 min	Gap release in rod group 4
1961.25	0 h 32 min	Failure of channel boxes around fuel bundles
2014.02	0 h 34 min	Gap release in rod group 5
3390.20	0 h 56 min	Time of total core uncover
3553.29	0 h 59 min	Collapse of fuel rods begins
3952.11	1 h 6 min	Core support structure fails in ring 1, Fuel rods collapse
4460.04	1 h 14 min	Core support structure fails in ring 2, Fuel rods collapse
8762.72	2 h 26 min	Start of containment venting through 362 rupture disc
14730.80	4 h 5 min	RPV lower head penetration in segment 2
14730.80	4 h 5 min	Beginning of debris ejection to cavity
14890.34	4 h 8 min	All water in RPV boiled away
15341.80	4 h 16 min	Core support structure fails in ring 5, Fuel rods collapse
15561.30	4 h 19 min	Core support structure fails in ring 3, Fuel rods collapse
15688.30	4 h 22 min	Core support structure fails in ring 4, Fuel rods collapse
100934.00	28 h 2 min	Cavity rupture/End of calculation
636.61		Hydrogen production from the core (kg)
905.69		Hydrogen production from the cavity (kg)
460.41		Total mass of hydrogen from zirconium
733.53		Total mass of radioactive material from the core
402.78		Total mass of radioactive noble gases released from the core (kg)
198.40		Total mass of radioactive Cs released from the core (kg)
40.55		Total mass of radioactive CsI released from the core (kg)

3.1.2 Temperatures and pressures

Figure 4 and Figure 5 present the temperatures and pressures in the core. Figure and Figure present the temperatures and pressures in different parts of the containment building.

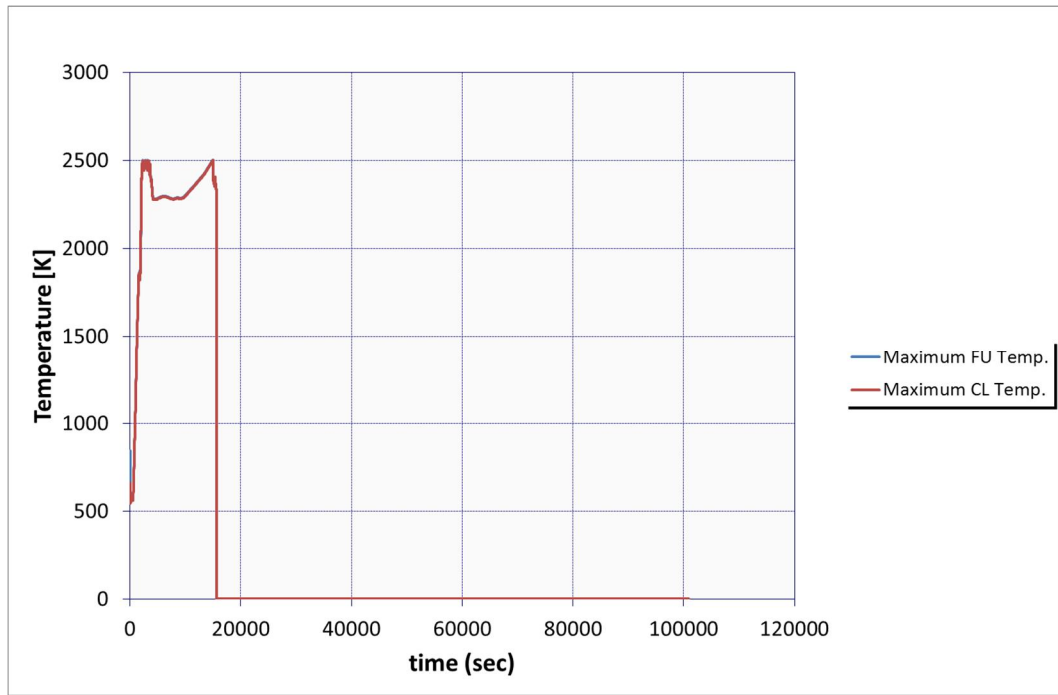


Figure 4. Maximum fuel (FU) and cladding (CL) temperatures

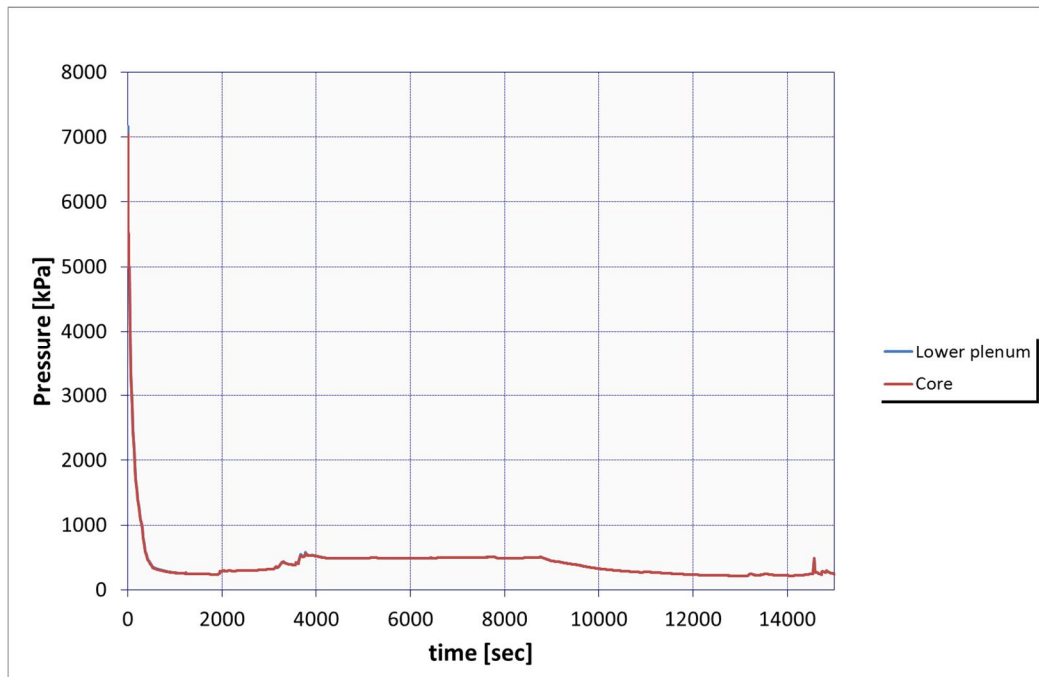


Figure 5. Lower plenum and core pressures

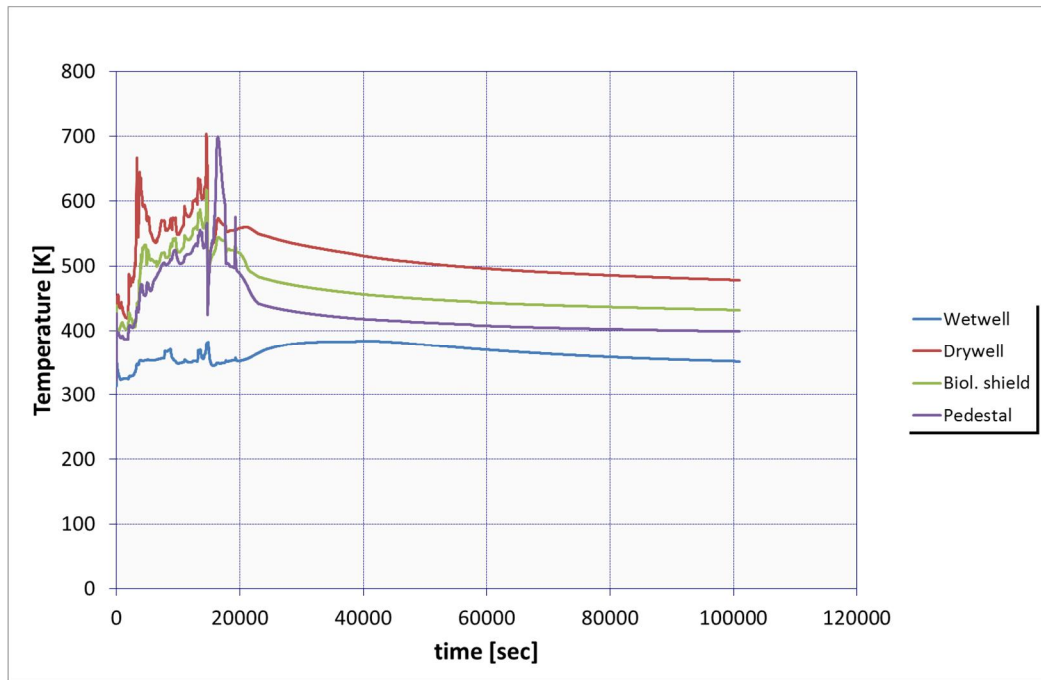


Figure 6. Temperatures in the containment building volumes

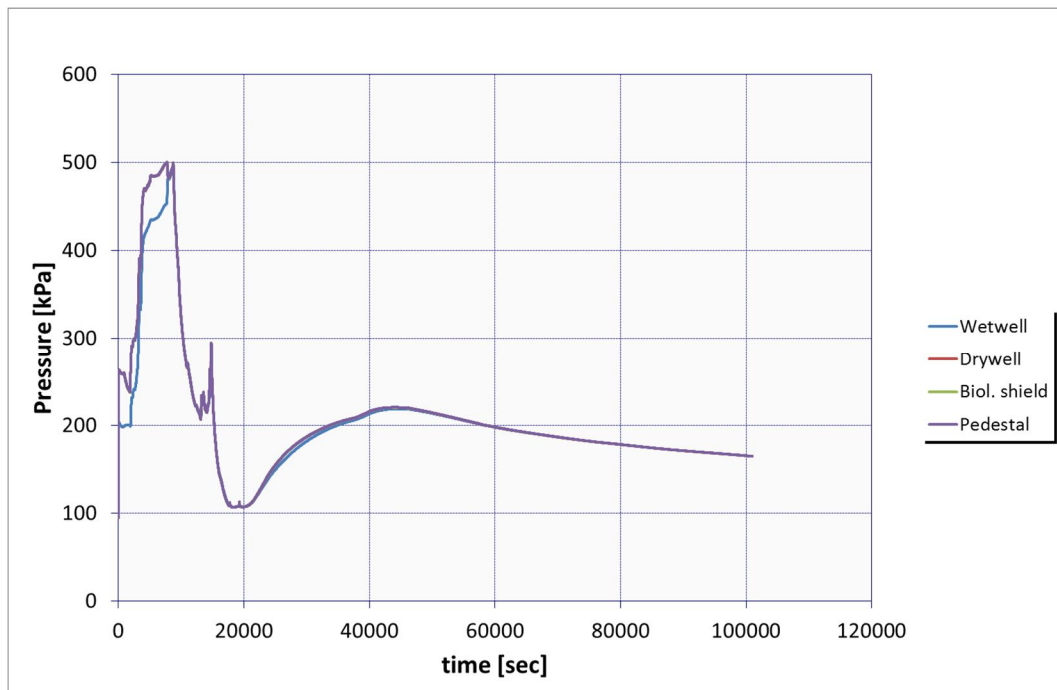


Figure 7. Pressures in the containment building volumes

Figure presents the core water level elevation. The times of the beginning of core uncover, time of total core uncover and the time of RPV emptying are marked in the figure.

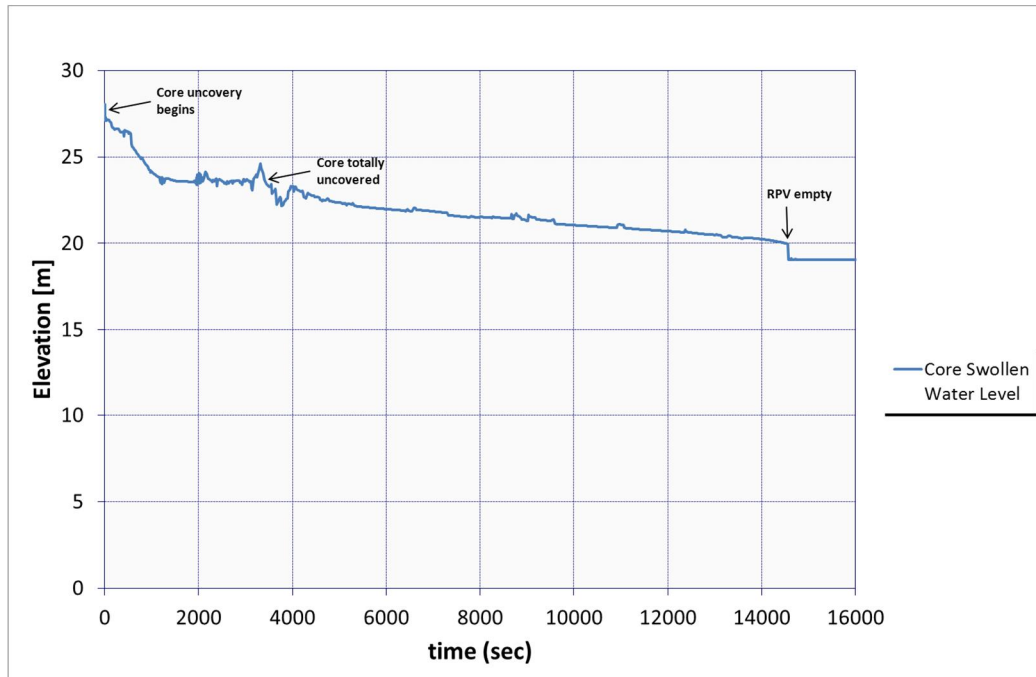


Figure 8. Core water level. Figure marks the places of core uncover and reactor pressure vessel (RPV) emptying.

Figure 9 presents the core decay heat power. The decay heat power in the beginning is 2500 MW, which is the normal operation power.

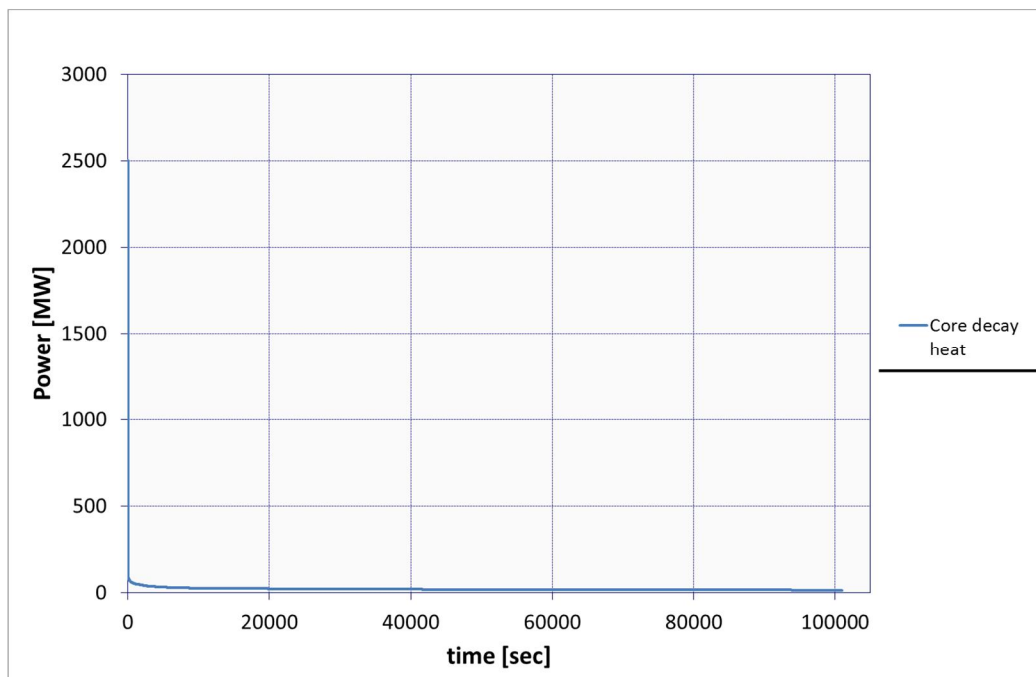


Figure 9. Core decay heat power

3.1.3 Masses

Figure 10 presents the total hydrogen mass produced in the core and in the cavity. The hydrogen production in the cavity begins after 17690 seconds, after the pressure vessel breach. Figure presents the total hydrogen mass from zirconium and figure 12 presents nitrogen masses in different volumes.

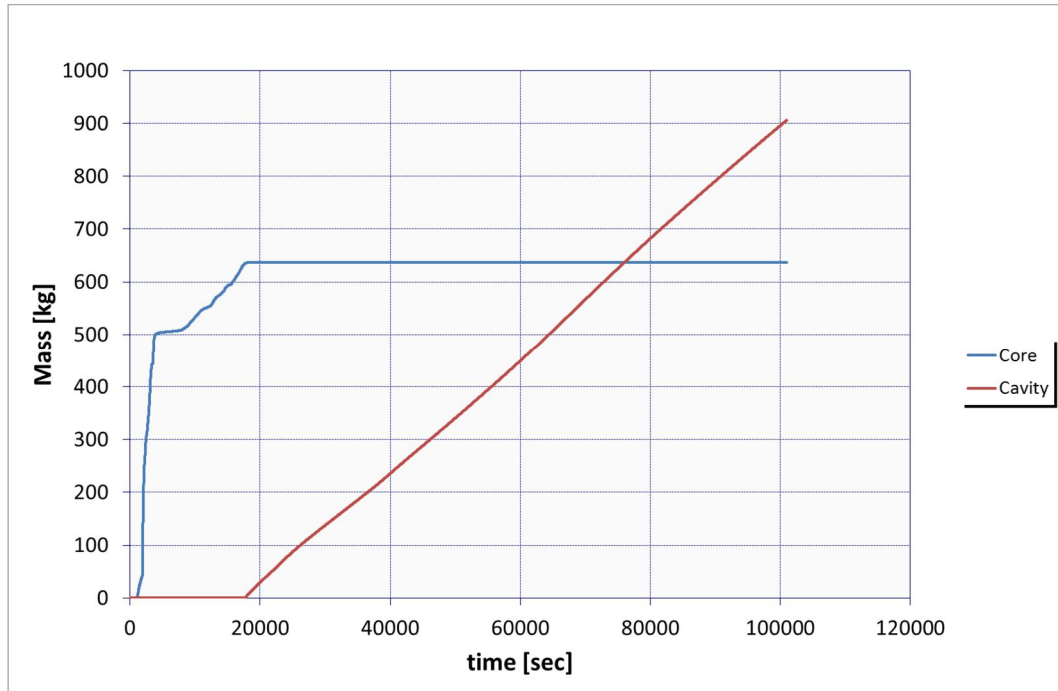


Figure 10. Total hydrogen mass produced in the core and in the cavity

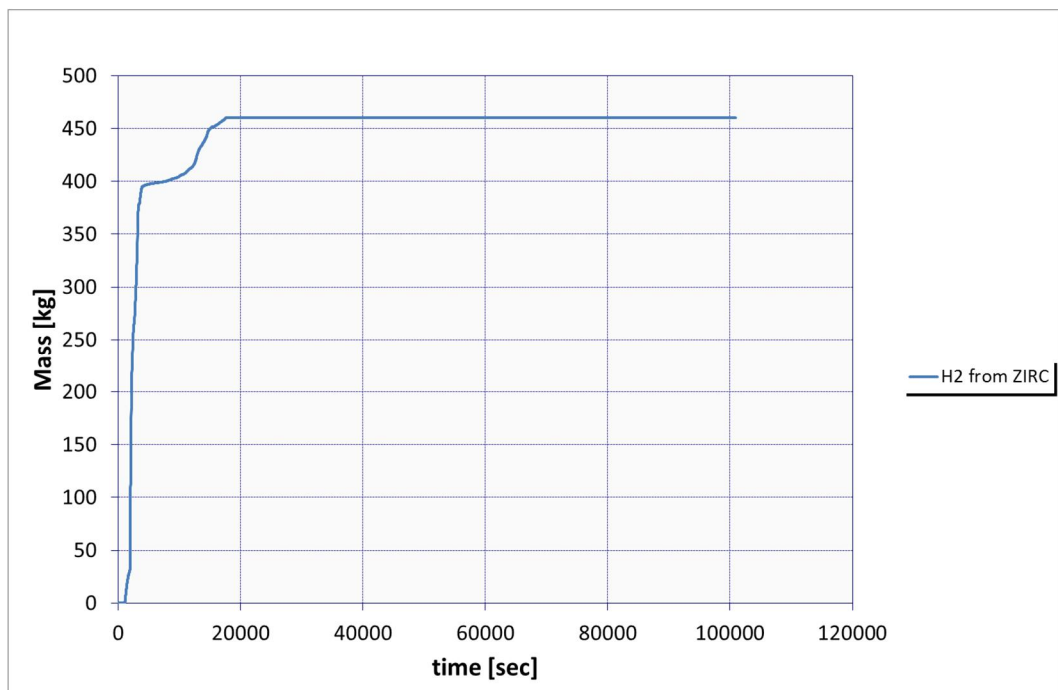


Figure 11. Total hydrogen mass from zirconium

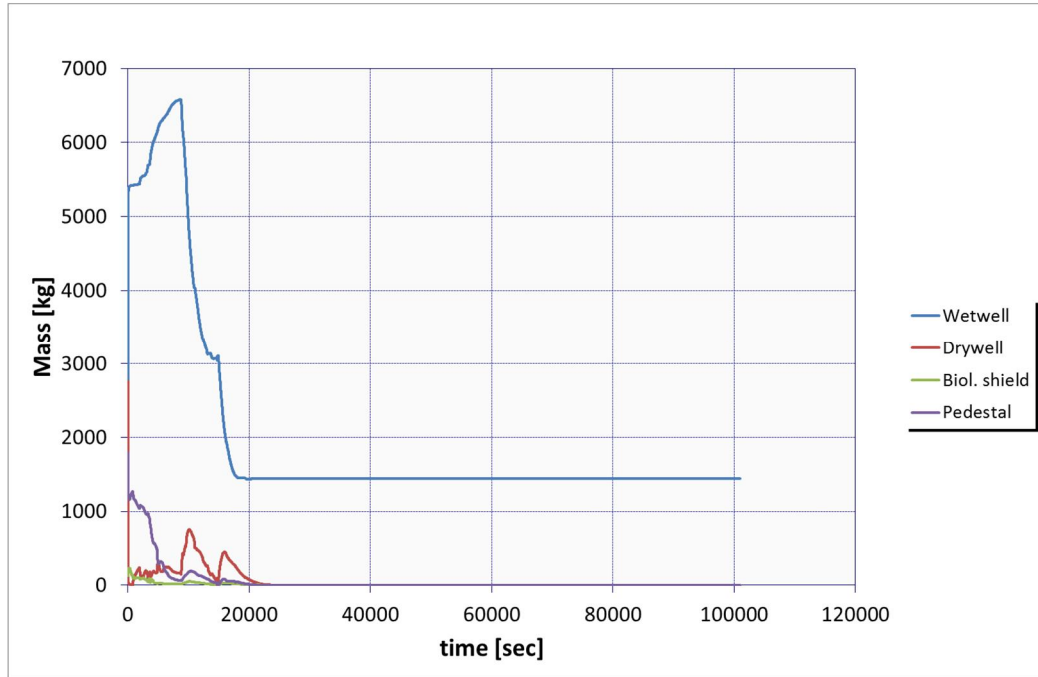


Figure 12. Nitrogen masses in different volumes

Figure 13 presents the water masses in the containment volumes. Masses are zero in other volumes except in wetwell and in the pedestal.

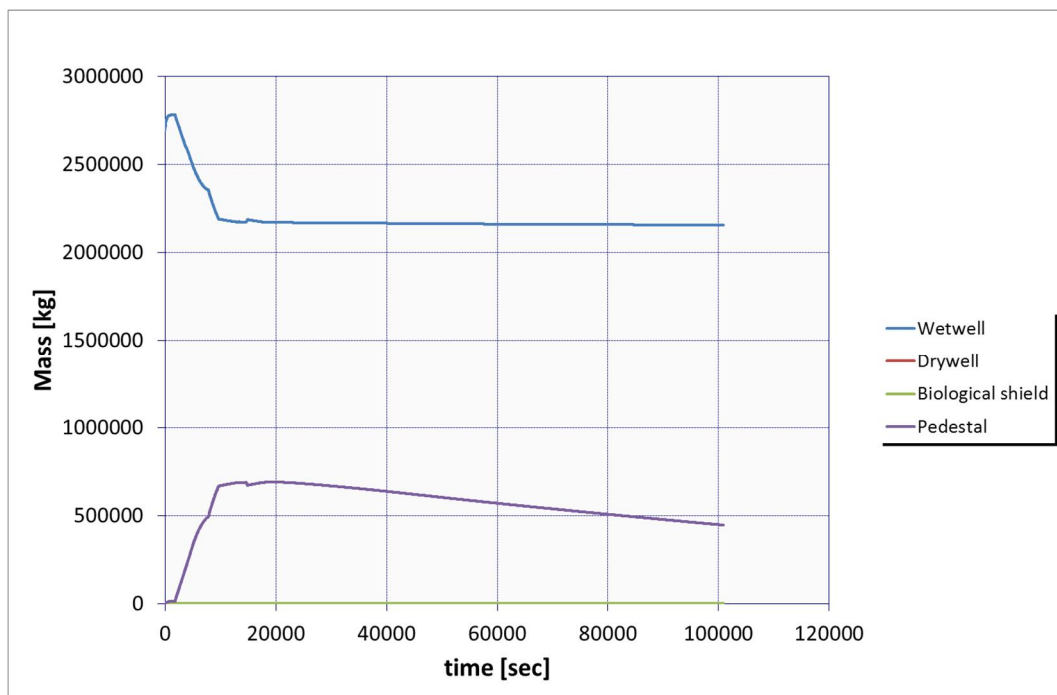


Figure 1. Water masses in different volumes

3.1.4 Radioactive releases

Figure 2 presents the total mass of radioactive material released from the core.

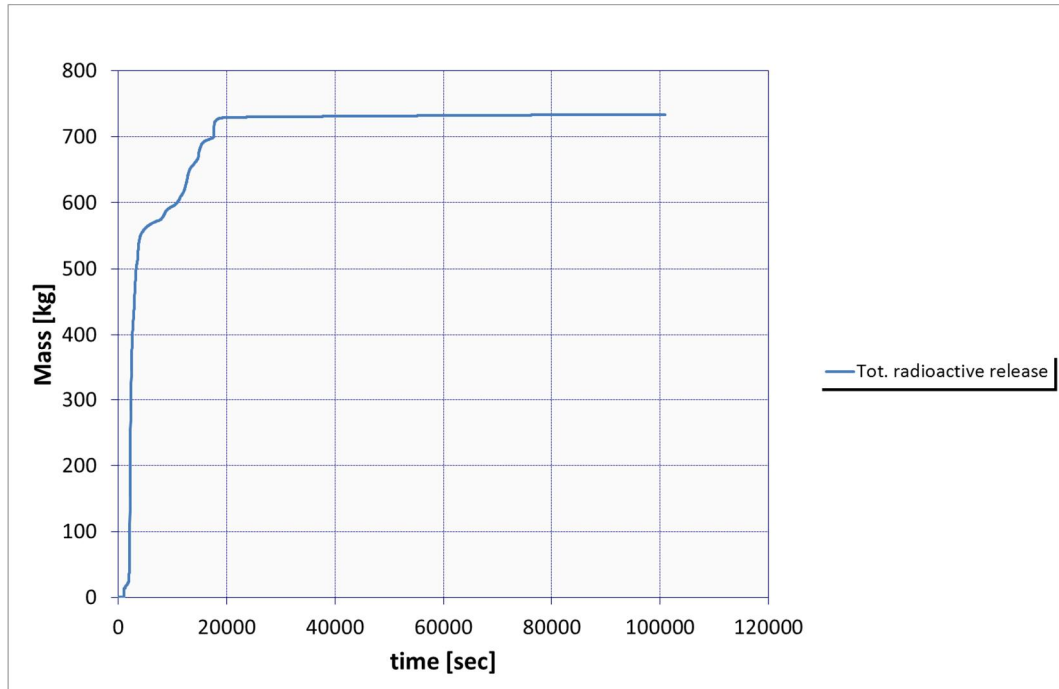


Figure 2. Total radioactive release from the core

Figure 3, Figure 4, Figure 5 and Figure 6 present the sums of all radioactive masses in all the volumes.

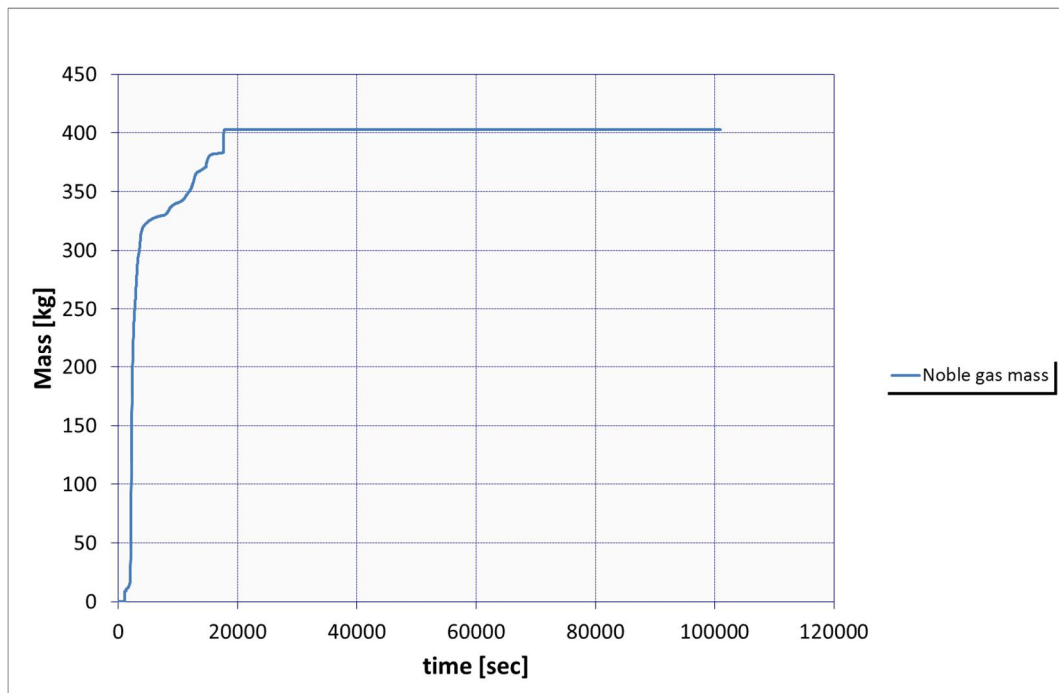


Figure 3. Sum of all radioactive noble gases in all the volumes

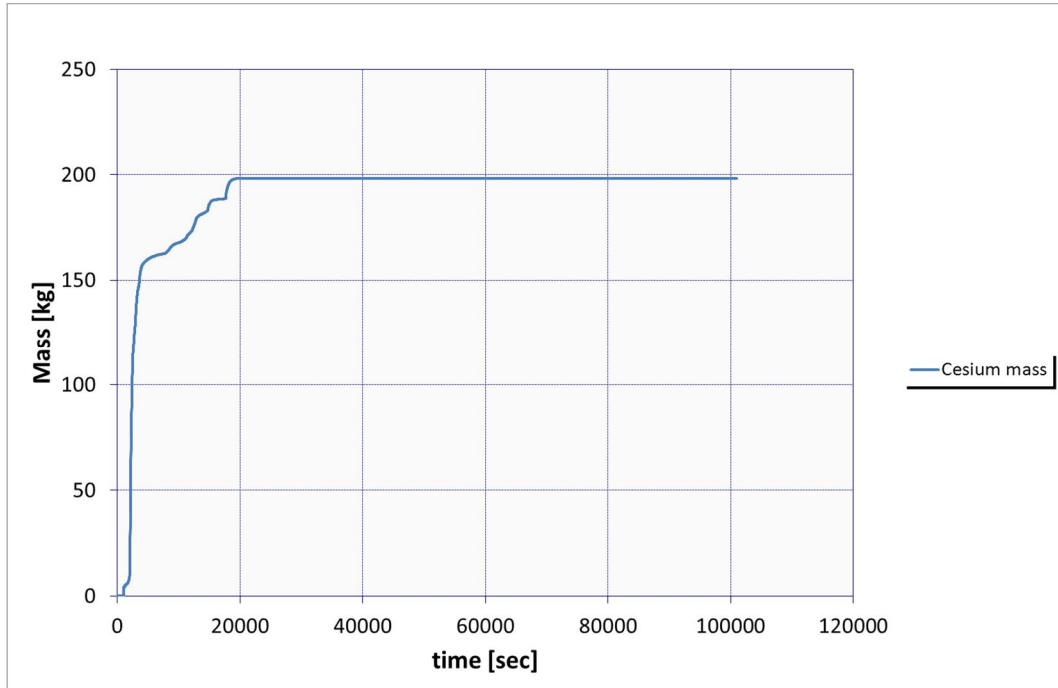


Figure 4. Sum of all radioactive Cesium masses in all the volumes

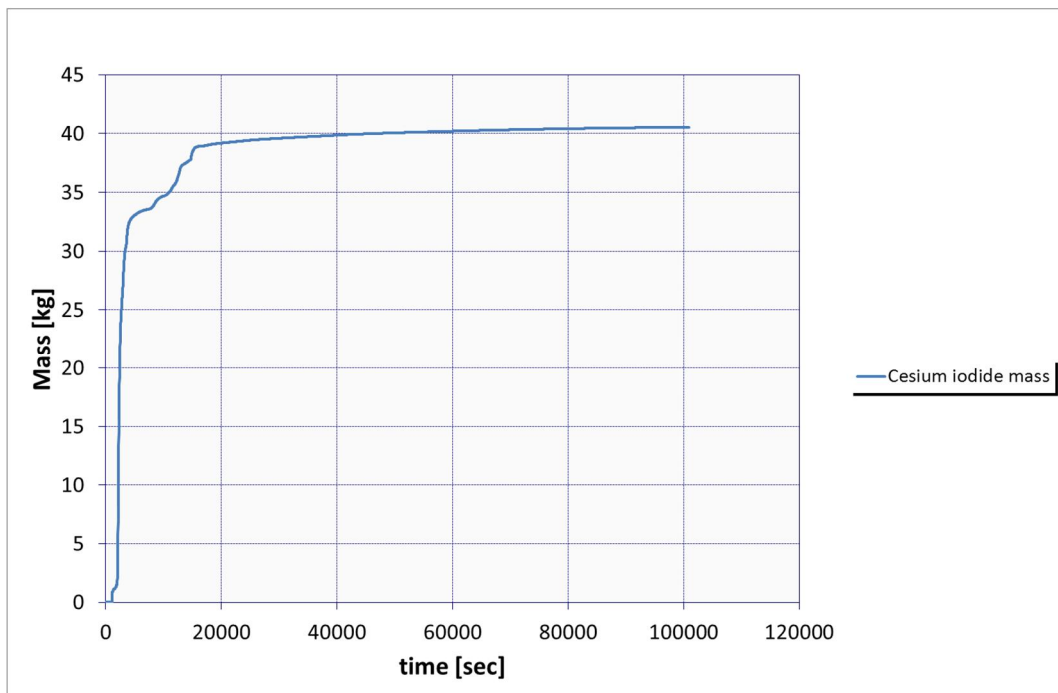


Figure 5. Sum of all radioactive cesium iodide masses in all the volumes

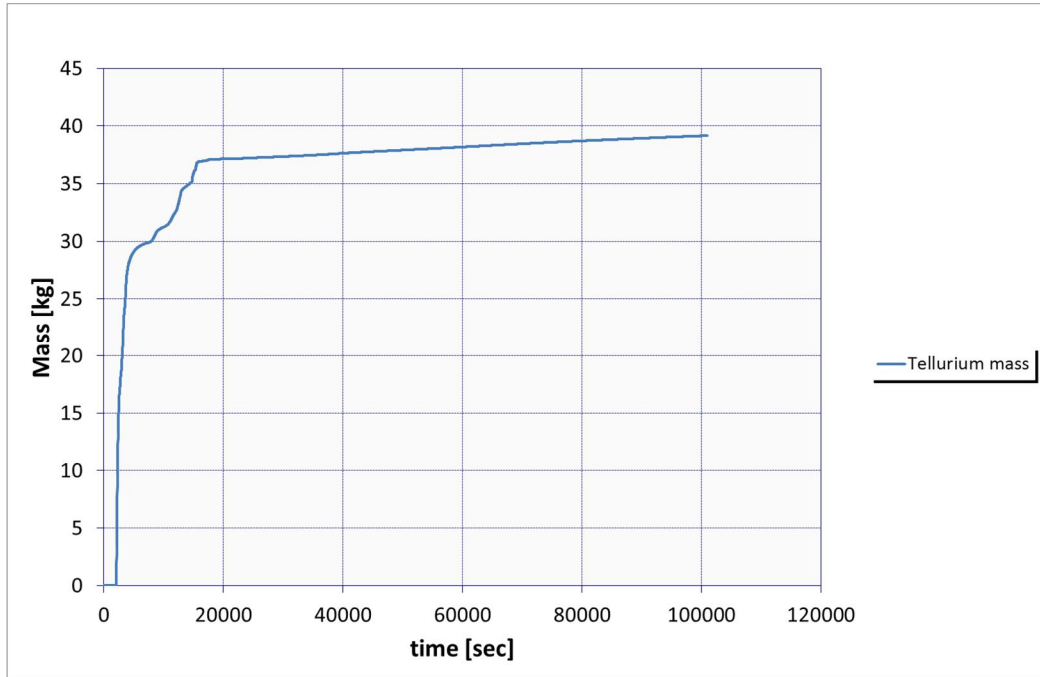


Figure 6. Sum of all radioactive tellurium masses in all the volumes

Figure 7 presents the noble gas vapour masses in different containment volumes. Figure , Figure , Figure , Figure , Figure and Figure present the cesium, cesium iodine and tellurium aerosol masses in gas and in water in different volumes.

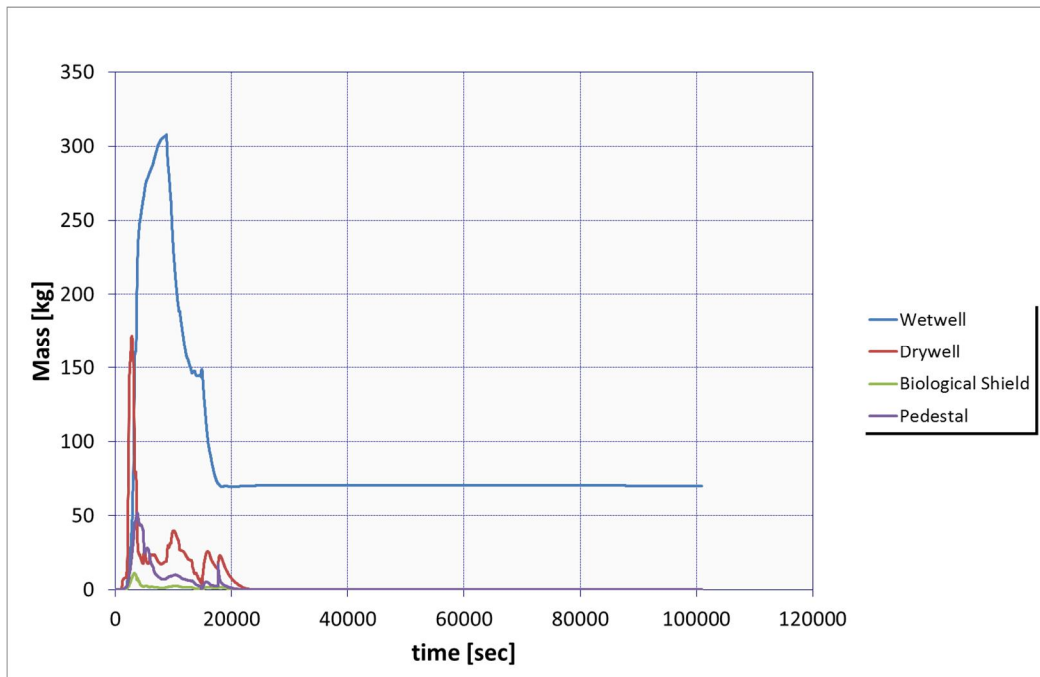


Figure 7. Noble gas vapor masses in different volumes

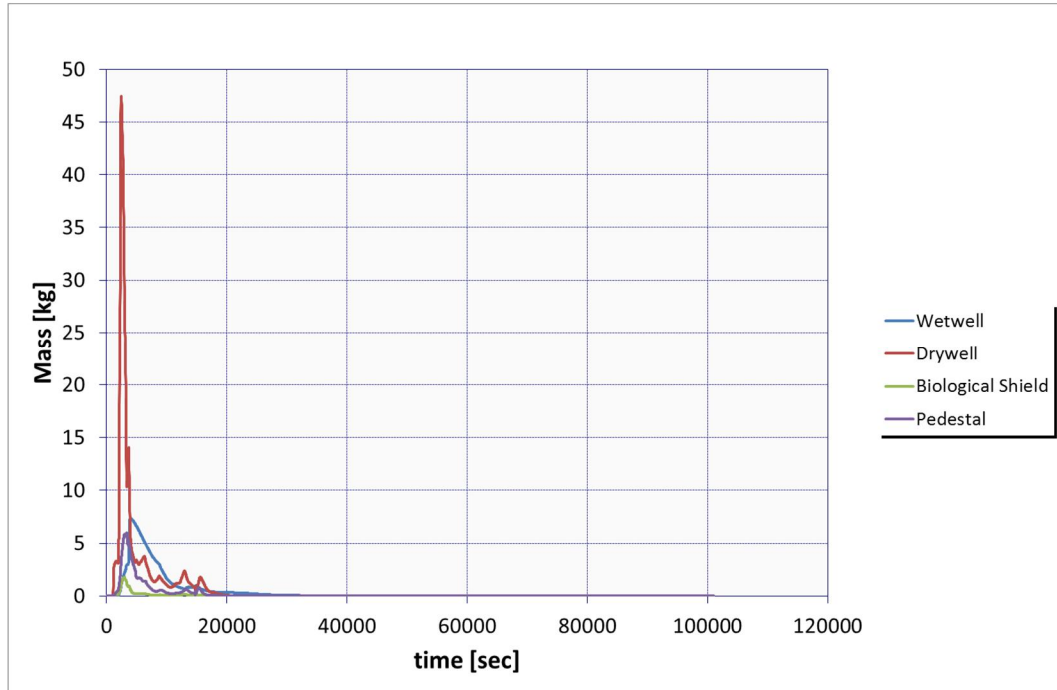


Figure 20. Cesium aerosol gas masses in different volumes

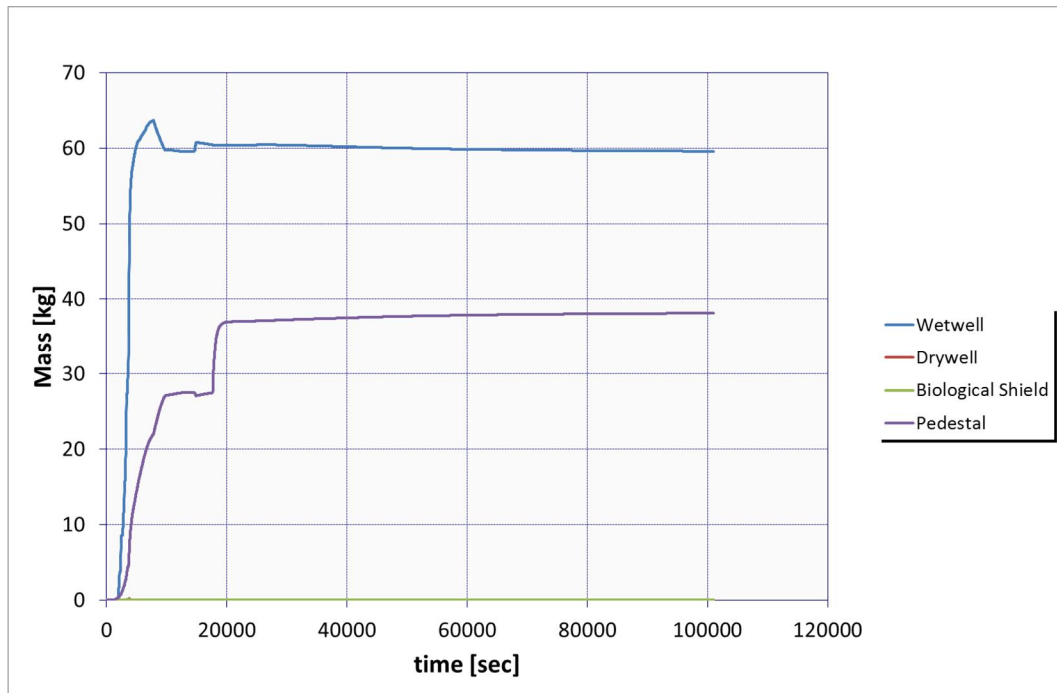


Figure 21. Cesium aerosol liquid masses in different volumes

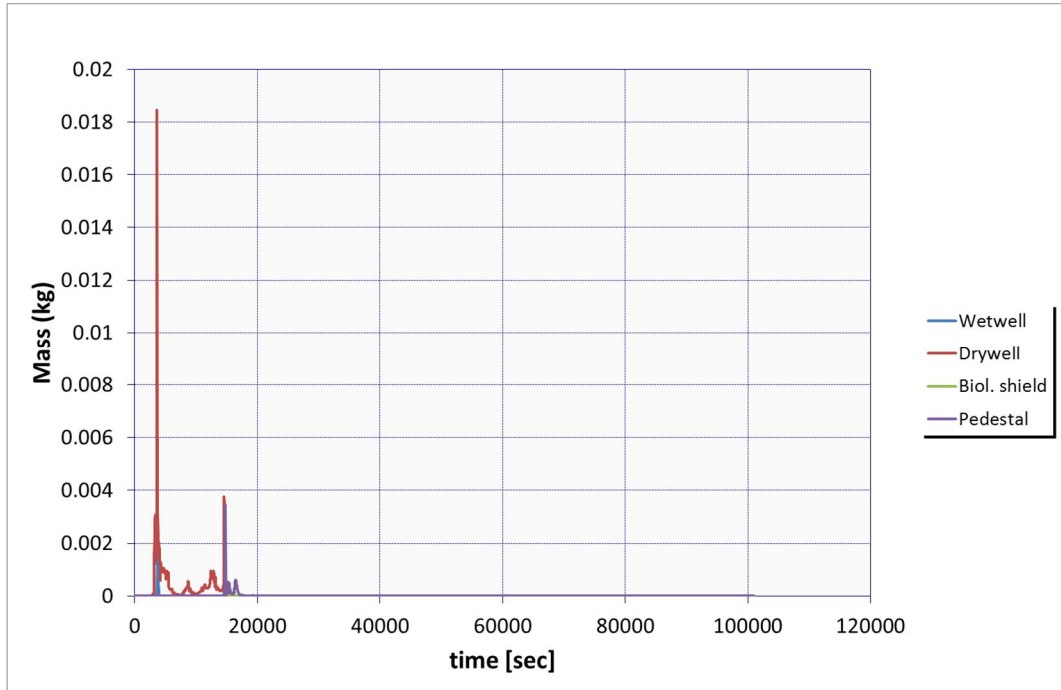


Figure 22. Cesium iodide gas masses in different volumes

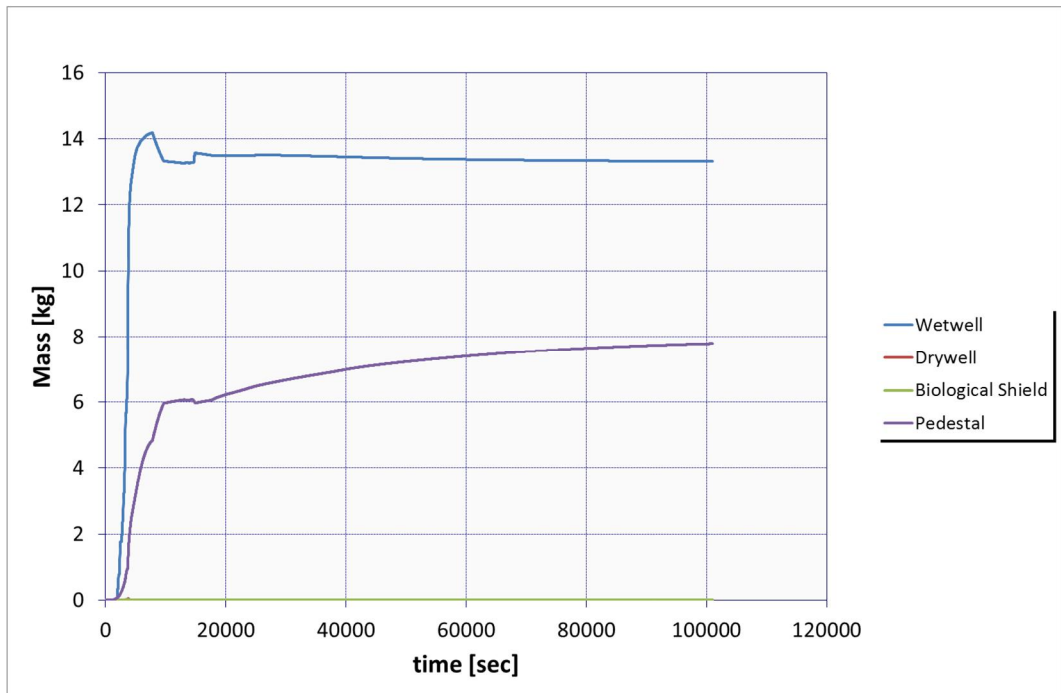


Figure 23. Cesium iodide liquid masses in different volumes

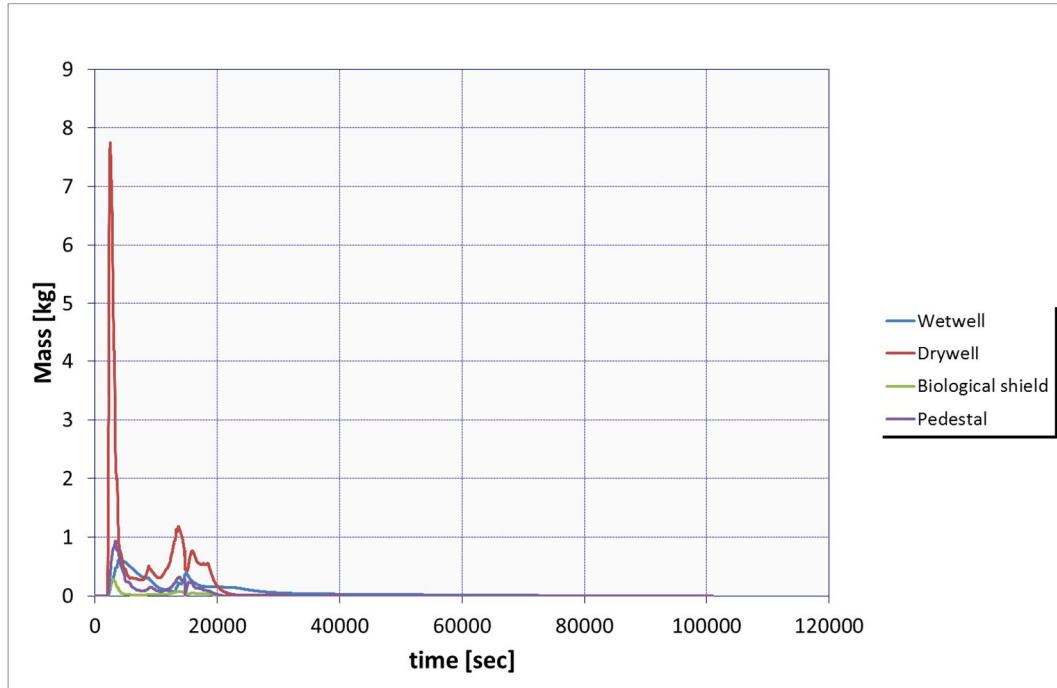


Figure 24. Tellurium gas masses in different volumes

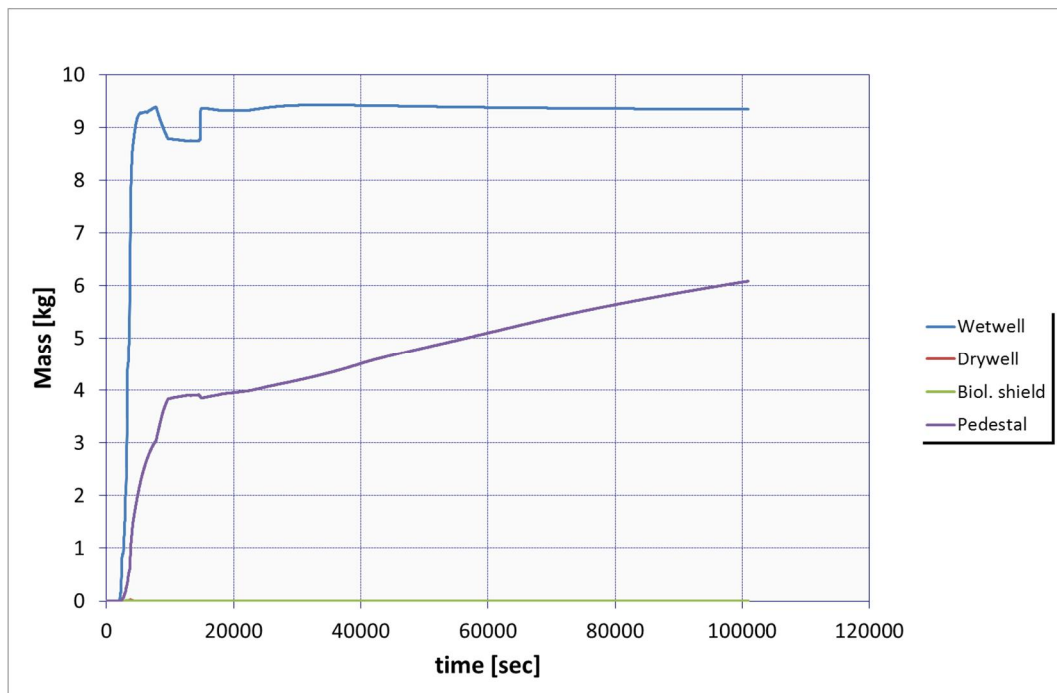


Figure 25. Tellurium liquid masses

Depositions of radioactive material on floor and on the walls are presented in Figure 8 and Figure 9 for drywell, Figure 10 and Figure 11 for wetwell, Figure and Figure for the pedestal and in Figure , Figure and Figure for the biological shield.

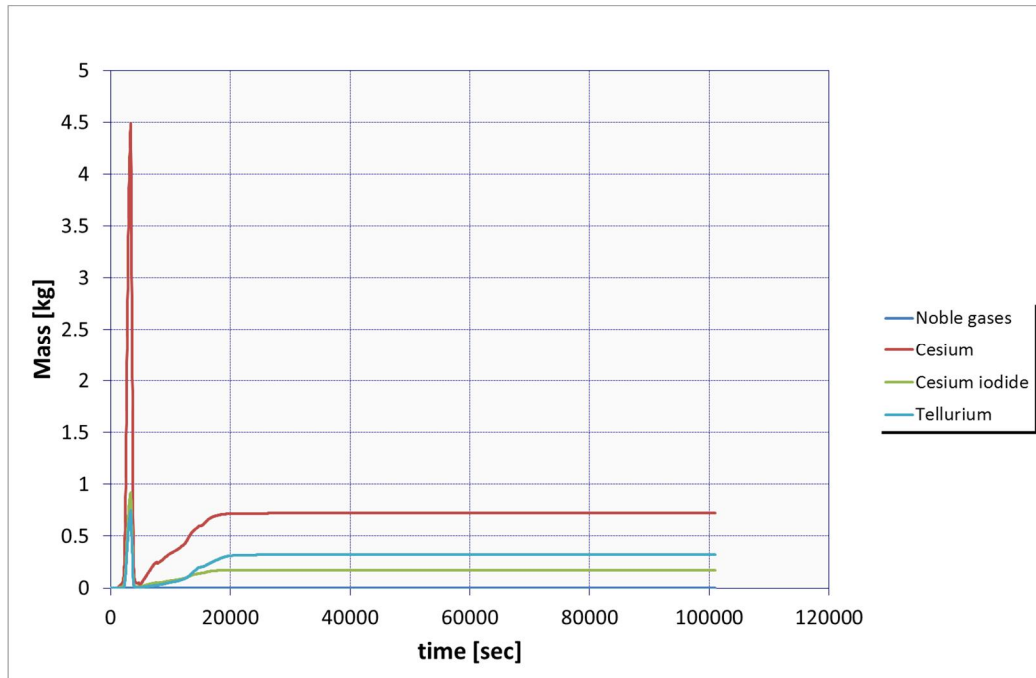


Figure 8. Depositions on drywell floor

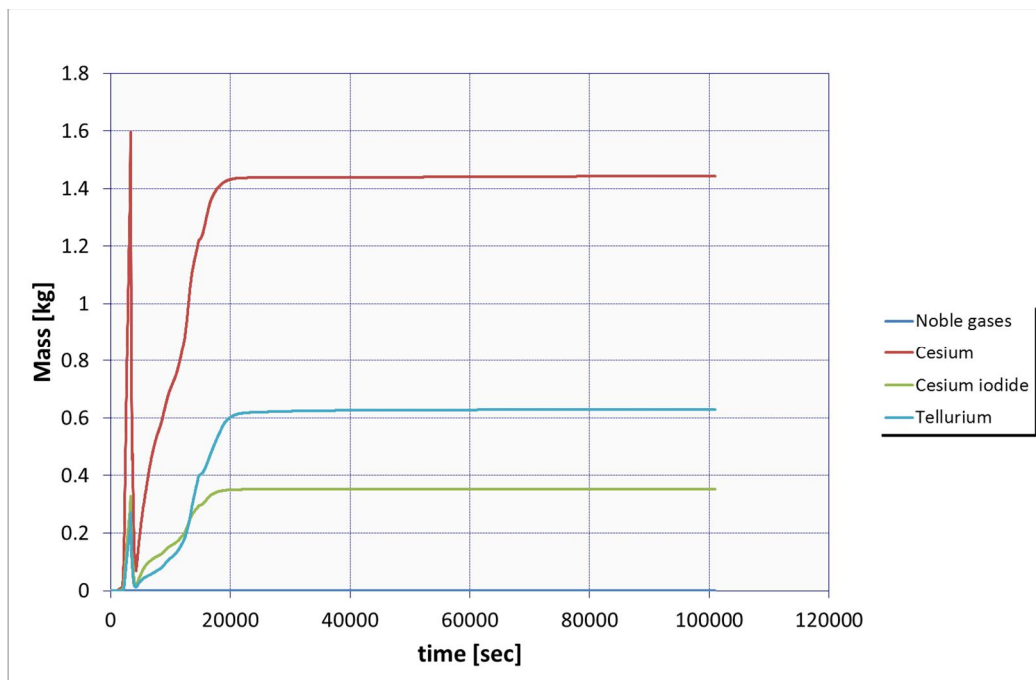


Figure 9. Depositions on drywell walls

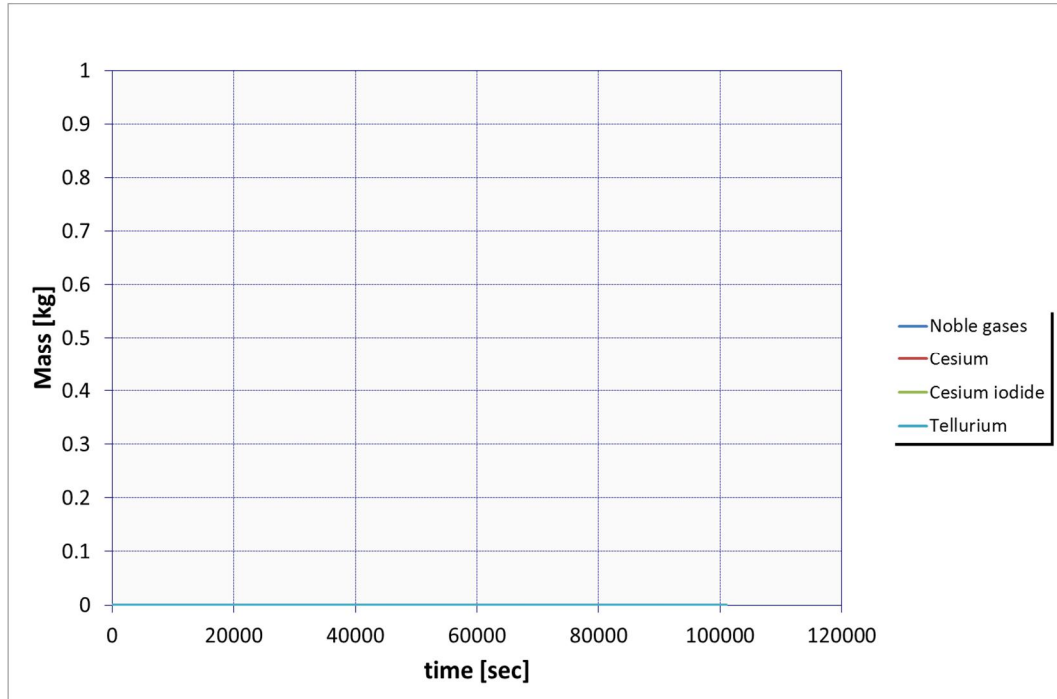


Figure 10. Depositions on wetwell floor. The amount is zero, because the floor is covered with water the whole time and therefore there can be no deposition.

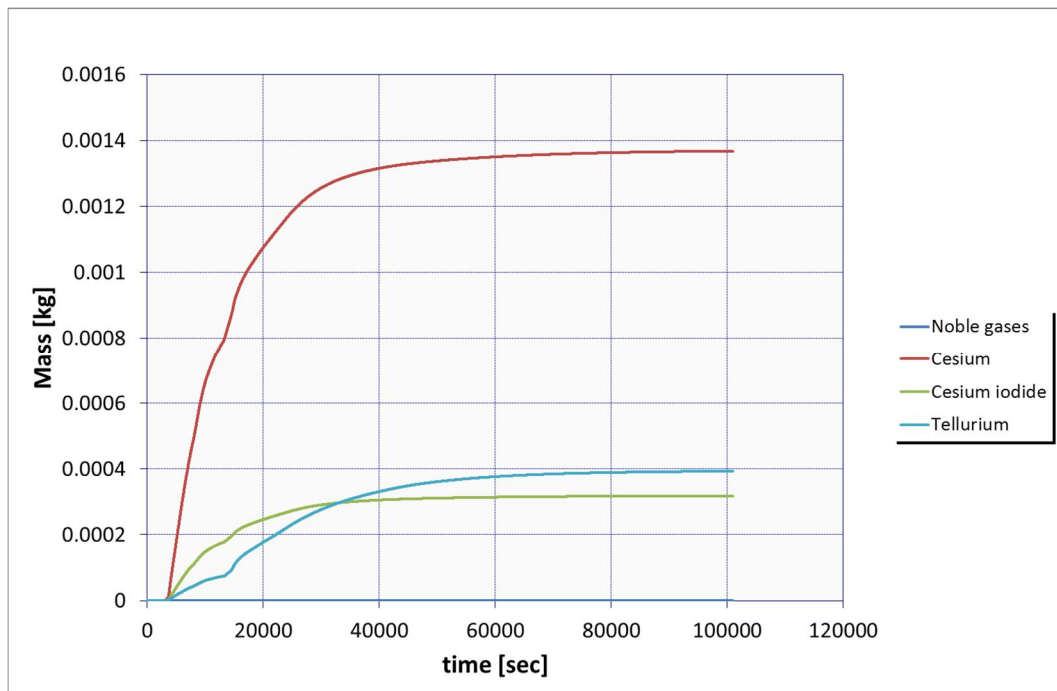


Figure 11. Depositions on wetwell walls

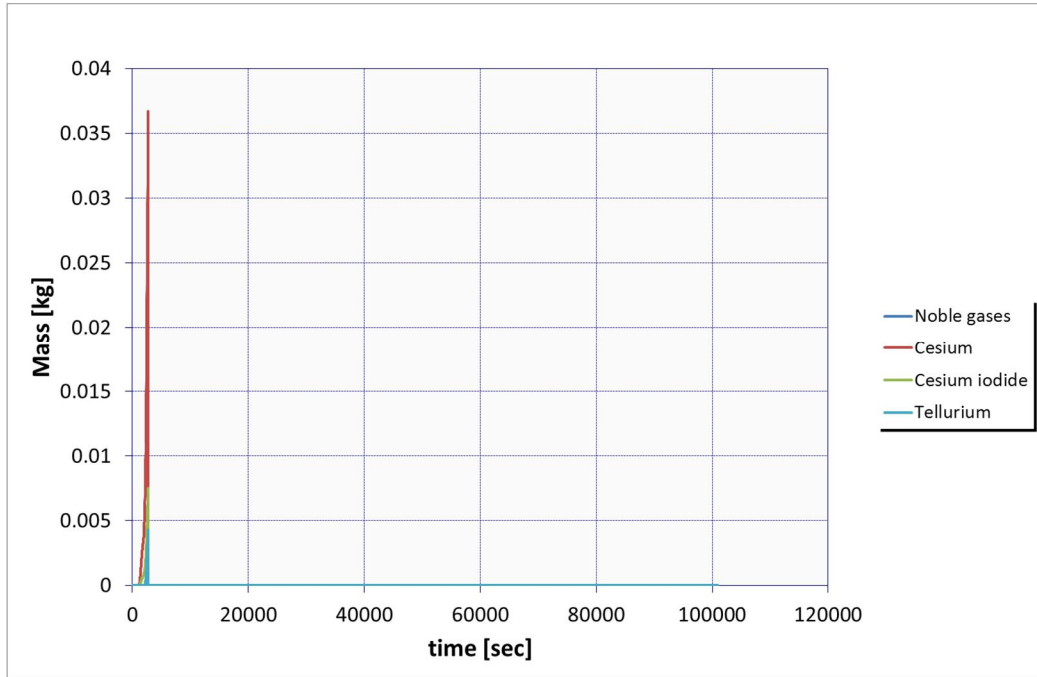


Figure 30. Depositions on pedestal floor

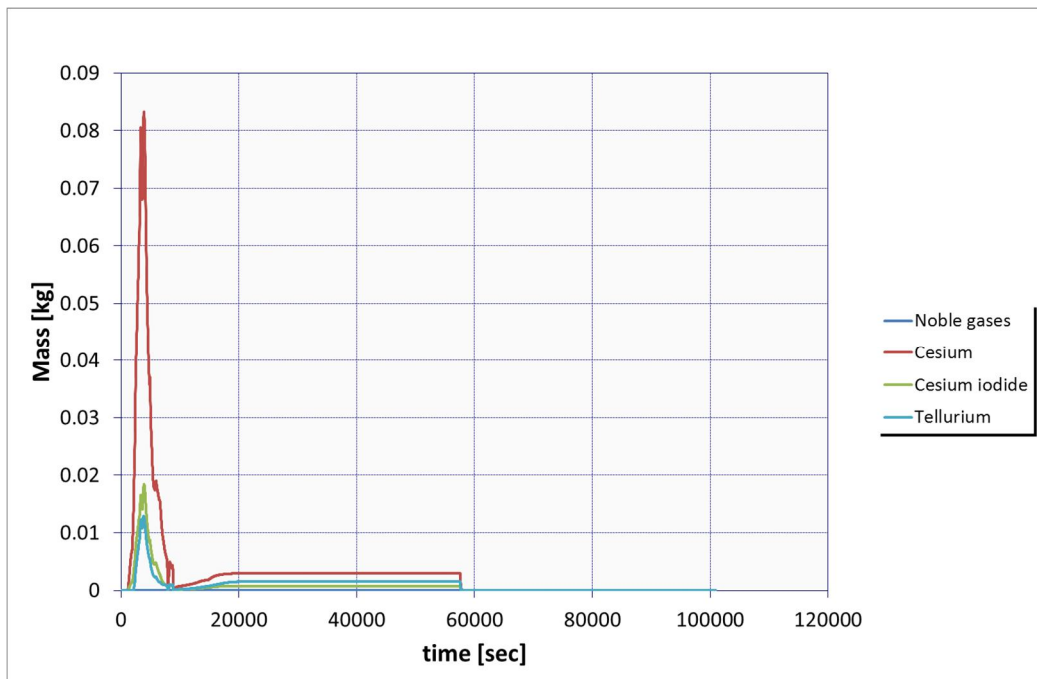


Figure 31. Depositions on pedestal walls

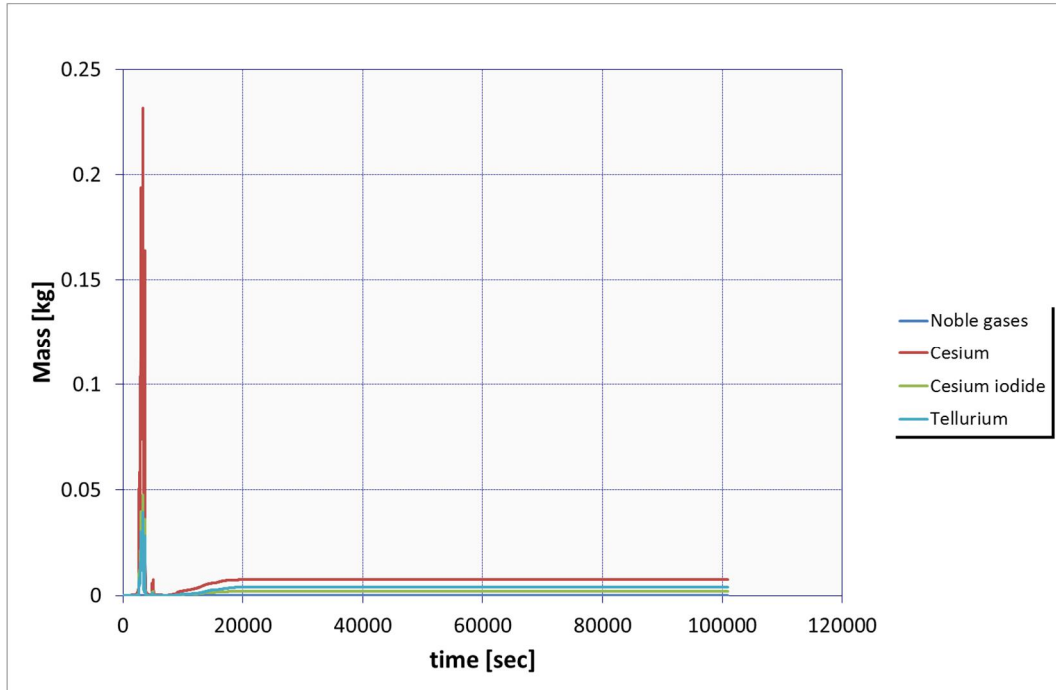


Figure 32. Depositions on biological shield floor

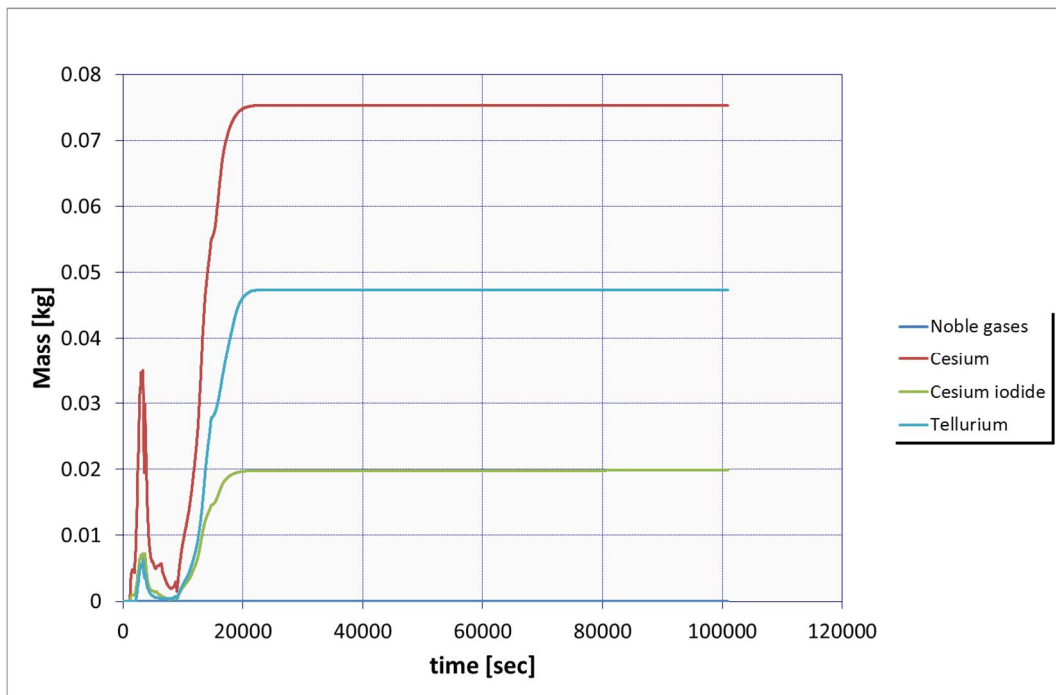


Figure 33. Depositions on biological shield lower wall (wall 1)

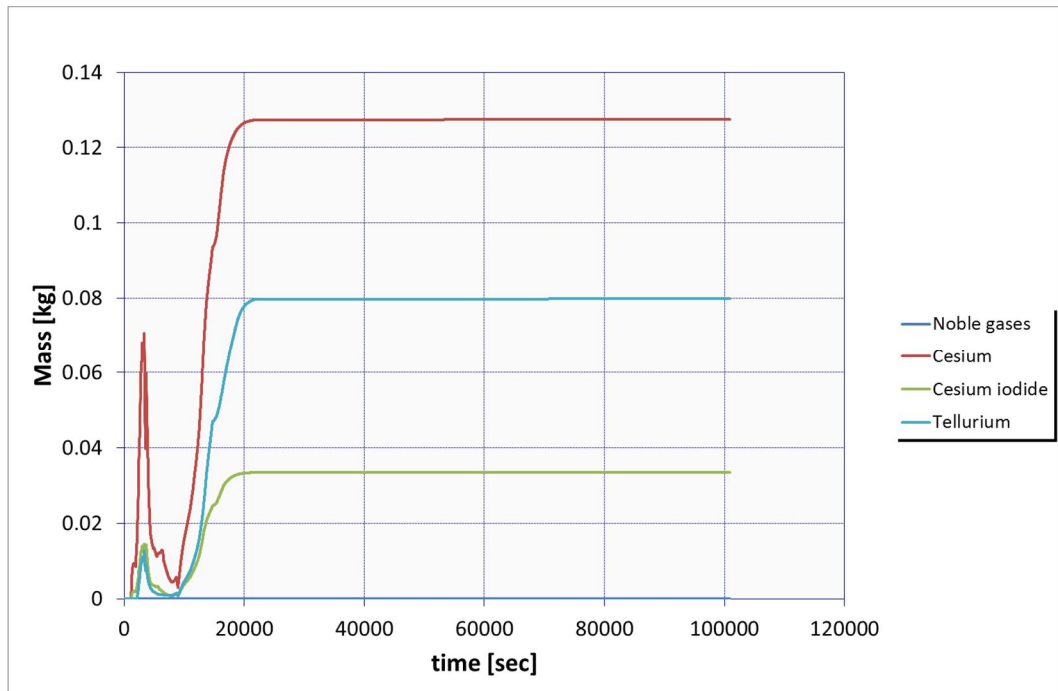


Figure 34. Depositions on biological shield upper wall (wall 2)

3.2 Dose results

In chapter 3.2.1 radiation doses are presented in the gas phases of wetwell, upper drywell, biological shield and lower drywell (pedestal). Doses in the water pools of the wetwell and pedestal from diluted radioactive material are presented in chapter 3.2.2, which also presents results for radiation from the core debris.

3.2.1 Doses in the gas phase

Gas phase volume in the containment fluctuates during the accident progress because water mass changes. Airborne nuclides and nuclides deposited on the surfaces are assumed to be smoothly dispersed in the air atmosphere volume.

Figure 35 illustrates the dose rates in the wetwell atmosphere and table 4 presents cumulative dose during time periods.

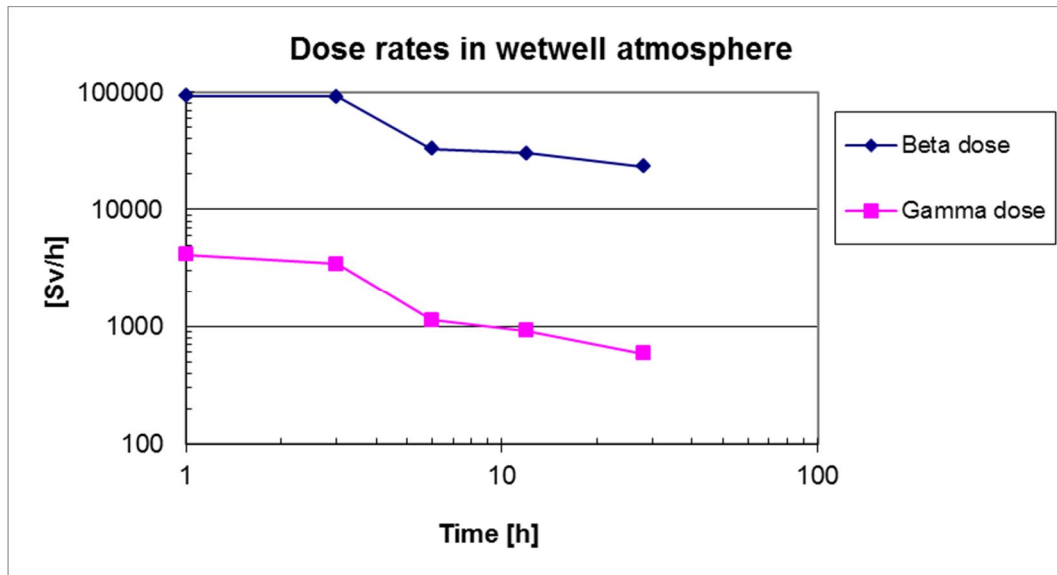


Figure 35. Dose rates in wetwell atmosphere.

Figure 35 shows that the maximum dose rate in the wetwell atmosphere is 93 000 Sv/h after one hour from the accident from beta radiation. Gamma dose rate is lower roughly with an order of magnitude. Table 4 shows that the cumulative dose during 27 hours is 1000 kSv. Beta dose makes up 97 per cent of this value.

Table 4. Cumulative dose [Sv] in wetwell atmosphere during time period.

	Time period				
	1...3 h	3...6 h	6...12 h	12...28 h	Total
Beta	1.8E+05	1.9E+05	1.9E+05	4.3E+05	9.9E+05
Gamma	7.6E+03	6.8E+03	6.1E+03	1.2E+04	3.3E+04

Figure 36 illustrates the dose rates in the drywell atmosphere and table 5 presents cumulative dose during time periods.

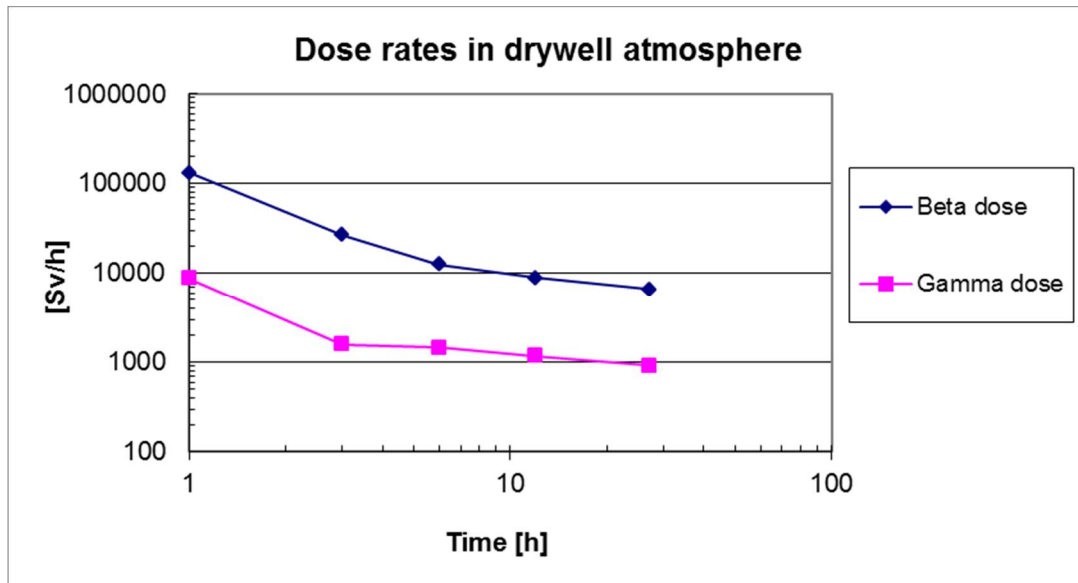


Figure 36. Dose rates in drywell atmosphere.

Figure 36 shows that the maximum dose rate in the drywell atmosphere is 130 000 Sv/h after one hour from the accident from beta radiation. Gamma dose rate is lower with an order of magnitude. Table 5 shows that the cumulative dose during 27 hours is 450 kSv. Beta dose makes up 91 per cent of this value.

Table 5. Cumulative dose [Sv] in drywell atmosphere during time period.

	Time period				Total
	1...3 h	3...6 h	6...12 h	12...28 h	
Beta	1.6E+05	5.9E+04	6.5E+04	1.2E+05	4.1E+05
Gamma	1.0E+04	4.6E+03	7.9E+03	1.7E+04	4.0E+04

Figure 37 illustrates the dose rates in the biological shield atmosphere and table 6 presents cumulative dose during time periods.

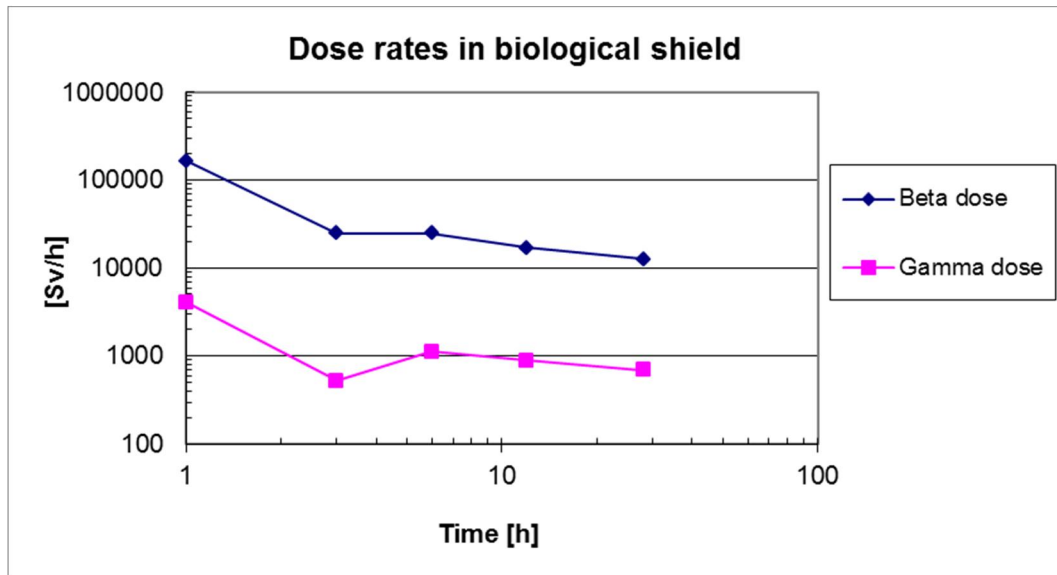


Figure 37. Dose rates in biological shield.

Figure 37 shows that the maximum dose rate in the biological shield atmosphere is 170 000 Sv/h after one hour from the accident from beta radiation. Gamma dose rate is lower with an order of magnitude. Table 6 shows that the cumulative dose during 27 hours is 660 kSv. Beta dose makes up 96 per cent of this value.

Table 6. Cumulative dose [Sv] in biological shield atmosphere during time period.

	Time period				
	1...3 h	3...6 h	6...12 h	12...28 h	Total
Beta	1.9E+05	7.5E+04	1.3E+05	2.4E+05	6.3E+05
Gamma	4.5E+03	2.5E+03	6.0E+03	1.3E+04	2.6E+04

Figure 38 illustrates the dose rates in the pedestal atmosphere and table 7 presents cumulative dose during time periods.

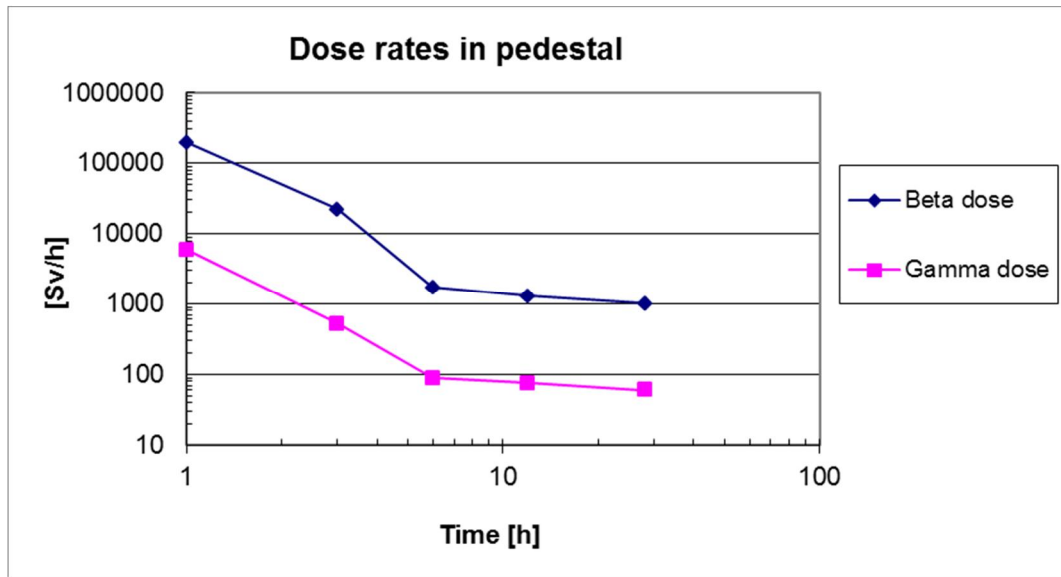


Figure 38. Dose rates in lower drywell (pedestal) atmosphere.

Figure 38 shows that the maximum dose rate in the pedestal atmosphere is 200 000 Sv/h after one hour from the accident from beta radiation. Gamma dose rate is lower with an order of magnitude. Table 7 shows that the cumulative dose during 27 hours is 290 kSv. Beta dose makes up 97 per cent of this value.

Table 7. Cumulative dose [Sv] in pedestal atmosphere during time period.

	Time period				
	1...3 h	3...6 h	6...12 h	12...28 h	Total
Beta	2.2E+05	3.6E+04	9.1E+03	1.8E+04	2.8E+05
Gamma	6.5E+03	9.1E+02	4.9E+02	1.1E+03	9.0E+03

3.2.2 Doses in the water pools

Radionuclides in the water are assumed to be smoothly diluted in the water volume.

Figure 39 illustrates the dose rates in the wetwell and pedestal water pools and table 8 presents cumulative dose during the time periods.

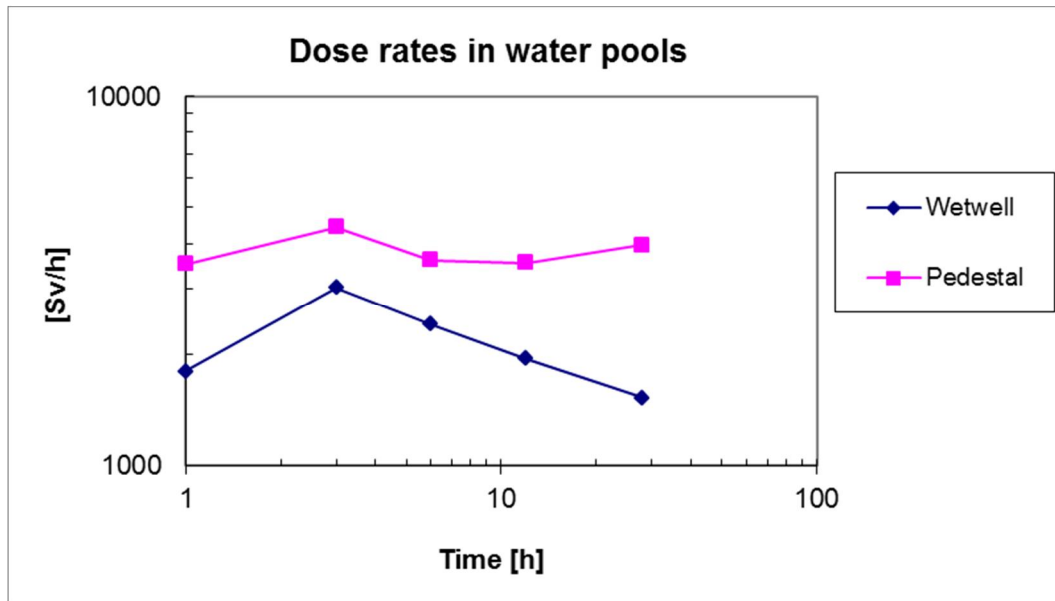


Figure 39. Dose rates in pools.

Figure 39 shows that the maximum dose rate in the wetwell water is 3 000 Sv/h after one hour from the accident. The maximum dose rate in the pedestal water is 4 400 Sv/h after one hour from the accident. Table 8 shows that the cumulative dose during 27 hours is 54 kSv in wetwell water and 100 kSv in pedestal water.

Table 8. Cumulative dose [Sv] in water pools during time period.

	Time period				
	1...3 h	3...6 h	6...12 h	12...28 h	Total
Wetwell	4.8E+03	8.2E+03	1.3E+04	2.8E+04	5.4E+04
Pedestal	7.9E+03	1.2E+04	2.1E+04	6.0E+04	1.0E+05

Figure 40 illustrates the dose rates in the pedestal water from the core debris on the bottom of the pedestal. It is assumed simply that noble gases, caesium, iodine and tellurium have left the core debris but the rest of the core inventory remains in the debris causing radiation.

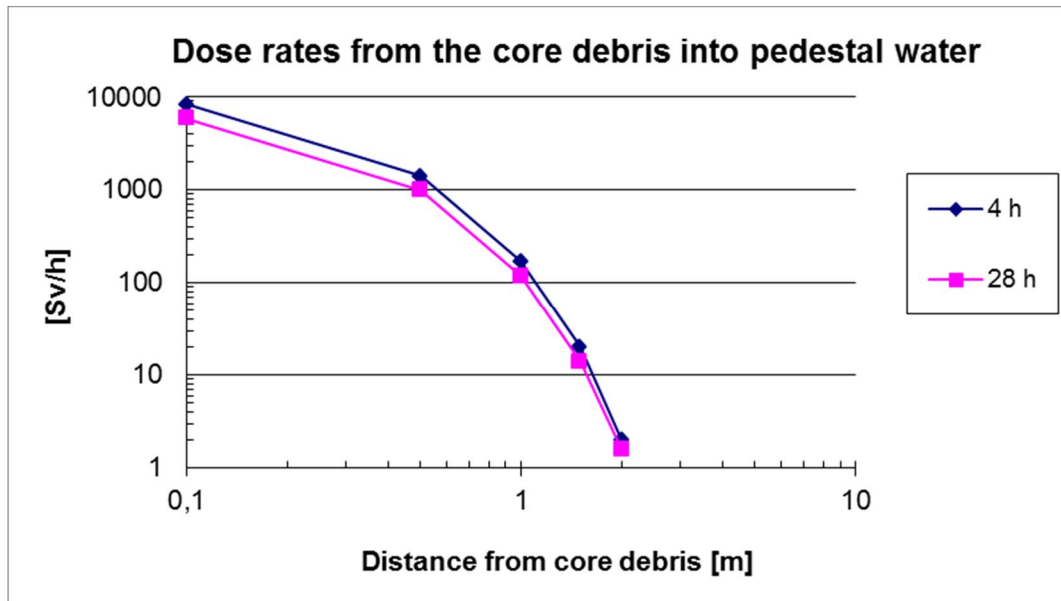


Figure 40. Dose rates in pedestal water as a function of distance to core debris.

Figure 40 shows that the dose rate decreases effectively as a function of distance from the debris surface. The maximum dose rate is 9 000 Sv/h at the distance of 0.1 m from the debris after 4 hours from the accident. At the distance of 0.5 m the dose rate is 1000 Sv/h and at the distance of 1.0 m the dose rate is about 100 Sv/h. Four hours is the time point when the pressure vessel failure takes place and the core melt drops down. The second time point of 28 h represents the end of the event because of the cavity breaks and MELCOR calculation stops.

Taking into account the attenuation of the radiation in water and the time period of 24 hours it can be estimated that the cumulative dose from the debris to water is approximately 52 kSv. Including the result from table 7 for pedestal the total dose to the pedestal water is 150 kSv during the event.

Figure 41 shows the fraction of gamma dose rate in the total dose rate in wetwell pool.

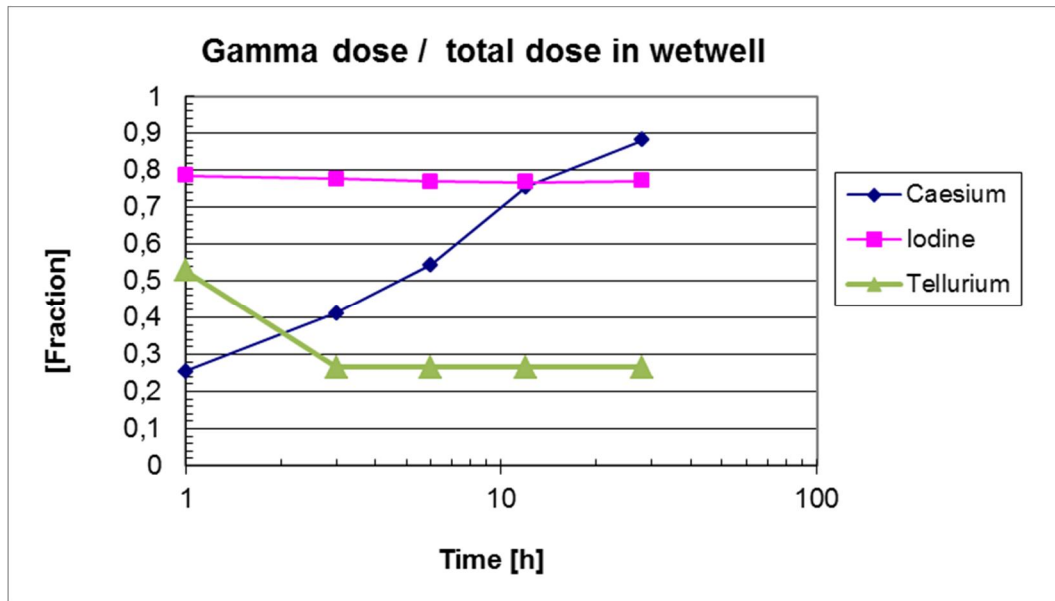


Figure 41. Fraction of gamma dose rate in the total dose rate in wetwell water.

Figure 41 illustrates that in the case of iodine group the gamma dose makes up constantly 80% of the total dose. The reversed trend is found for tellurium, in which case beta radiation dominates the dose after one hour. In the case of caesium beta radiation dominates the dose up to 5 hours but at a later phase gamma radiation dominates the dose.

It can be roughly estimated that about 70% of the total dose in wetwell water is caused by the gamma radiation. Due to contribution of the gamma radiation from the core debris to the pedestal water, the contribution from the gamma radiation is about 80% in pedestal.

3.3 ChemPool results

The radiation G value for nitric acid formation in water phase, $G(\text{HNO}_3) = 0.007$ molecules/100 eV [Beahm et al. 1992], was used in the ChemPool calculations. The HCl formation amount was taken from the report [Leppämäki et al.]. It was assumed that 25% of the total amount of HCl was released. The amount of HCl released was 117.5 kg.

Table 9 shows the ChemPool definitions for HCl formations in Pedestal and HNO_3 formations in Wetwell and Pedestal. These values are taken from Dose results in Chapter 3.2. The total amount HNO_3 released in wetwell and pedestal were 8,7 kg and 5,6 kg. These records are only table definitions containing time steps and rate values in given time intervals. Table 10 shows how these rates are actually mapped to specific species and pools.

Table 9. ChemPool definitions for HCl and HNO₃ formations rates

TF71000	'HCl Pedestal'	4	1.0	0.0
*	Time [s]		Formation rate [kg/s]	
TF71010		0.00000		0.0
TF71011		3600.00		0.652778
TF71012		3780.00		0.0
TF71013		100800.		0.0
*				
TF72000	'HNO3 WetWell'	6	1.0	0.0
*	Time [s]		Formation rate [kg/s]	
TF72010		0.00000		0.0
TF72011		3600.00		0.000107395
TF72012		10800.0		0.000122311
TF72013		21600.0		9.6954E-05
TF72014		43200.0		7.8309E-05
TF72015		100800.		0.0
*				
TF73000	'HNO3 Pedestal'	6	1.0	0.0
*	Time [s]		Formation rate [kg/s]	
TF73010		0.00000		0.0
TF73011		3600.00		6.06016E-05
TF73012		10800.0		6.13687E-05
TF73013		21600.0		5.36976E-05
TF73014		43200.0		5.75331E-05
TF73015		100800.		0.0

 Table 10. ChemPool definitions for HCl and HNO₃ pool locations

*				
*	REACTIONS			
*				

*				
CP10100	HCL	400	710	* name (32 chars), CV no, TF no 300 Drywell
CP10200	HNO3	200	720	* name (32 chars), CV no, TF no 200 Wetwell
CP10300	HNO3	400	730	* name (32 chars), CV no, TF no 400 Pedestal

Figures 42-45 shows the pH values as function of time with the given HCl and HNO₃ formation rates and with H₂O(g), N₂(g), O₂(g), H₂(g), CO(g), CO₂(g) H₂O(a), CsOH, CSI masses calculated by MELCOR.

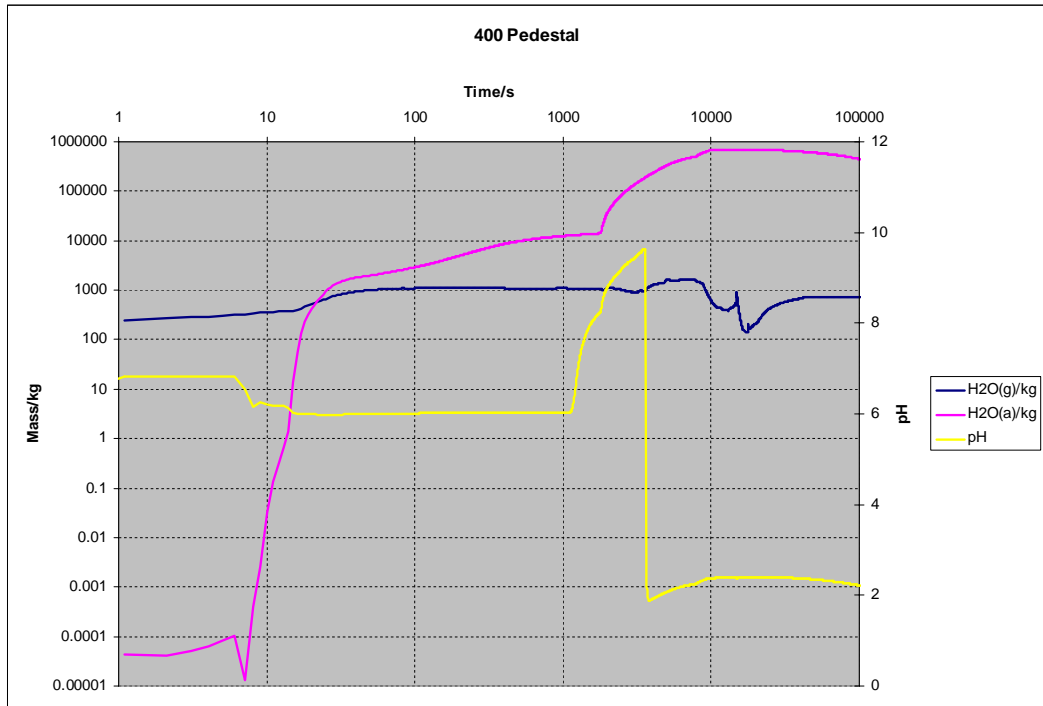


Figure 42. Water vapour and water mass and pH in Pedestal

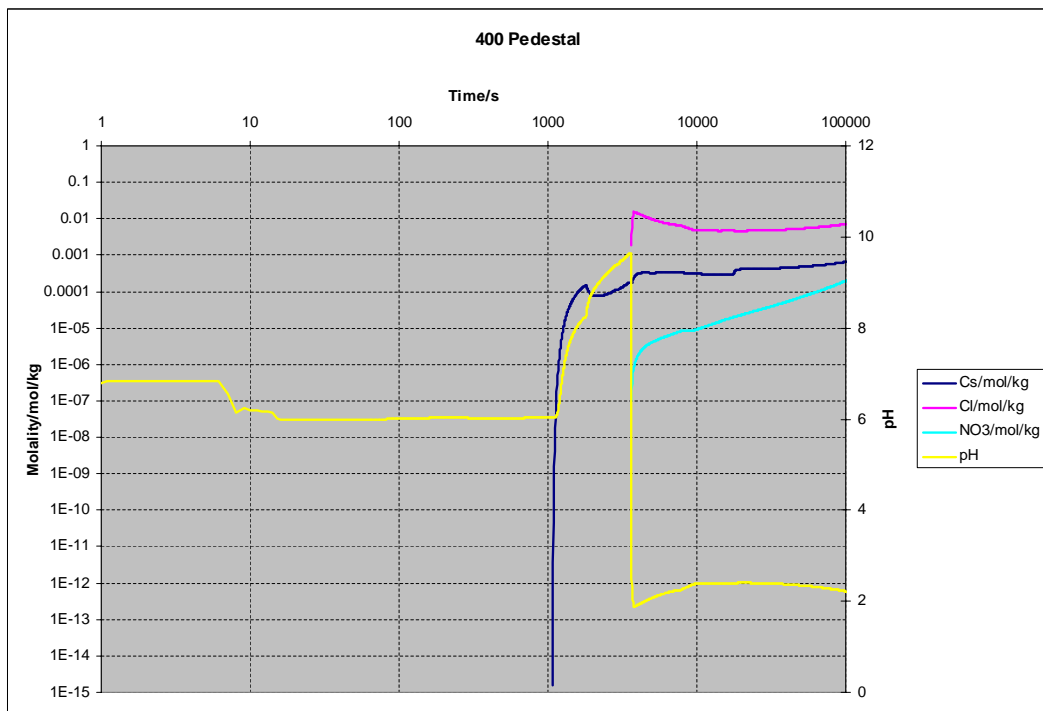


Figure 43. Cesium (CsOH), Chlorium (HCl), Nitrate ion (HNO_3) and pH in Pedestal.

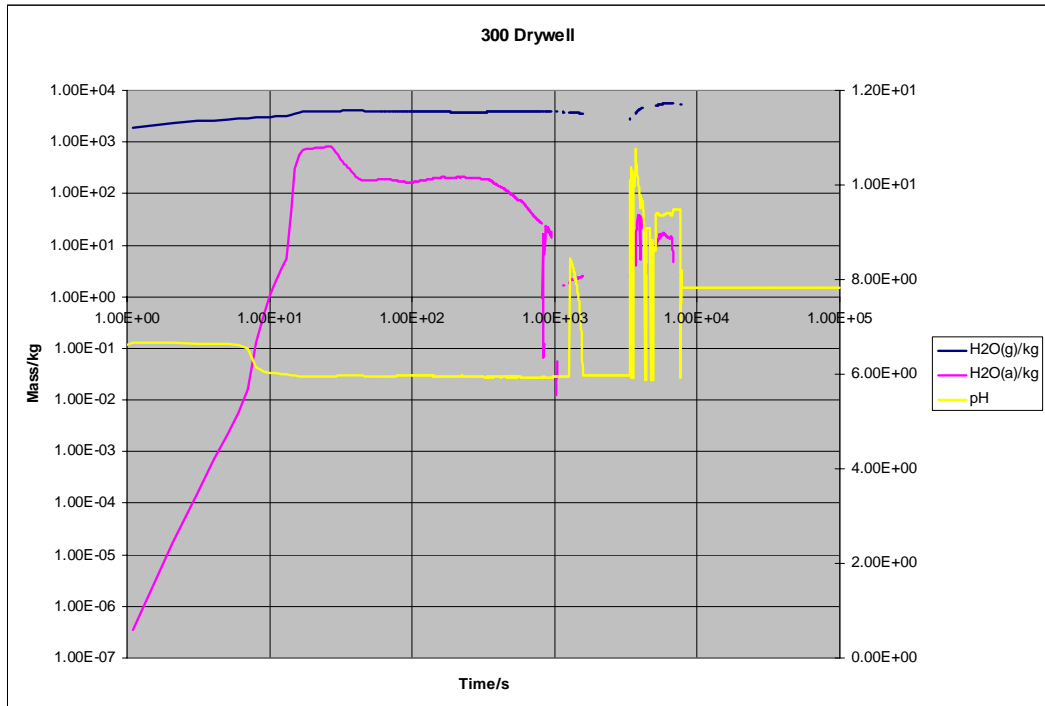


Figure 44. Water vapour and water mass and pH in Drywell

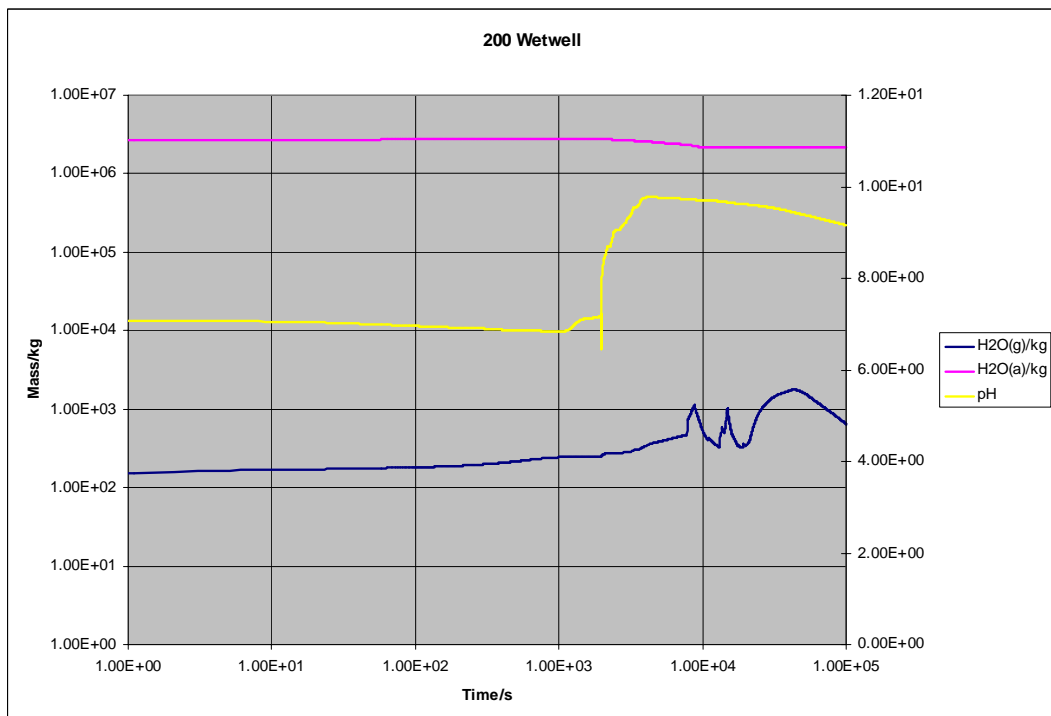


Figure 45. Water vapour and water mass and pH in Wetwell

4 Conclusions and Summary

The accident scenario was a basic LOCA scenario and a break in the BWR main steam line. This accident results in core melt and a significant fraction of the radioactive material is released to the containment. Input data for radiation dosage calculations was obtained by the MELCOR calculation, in which spreading of the radioactive material in different volumes of the containment was determined. Accident sequence was followed until core debris melted a hole in the reactor cavity.

Doses of the most significant radioisotopes in the containment gas phase and water pools were calculated using appropriate approaches. Time dependent isotope concentrations were obtained by the ORIGEN2 code. The nitric acid formation and the amount of HCl released were calculated and pHs of water pools were calculated using a new developed ChemPool program. The formation of nitric acid in pedestal pool was 5.6 kg and in wetwell pool 8.7 kg. In water pool of pedestal most of the acid is coming from cables in form of HCl, 117.5 kg. Due this the pH drops rapidly to 2. The influence of nitric acid is small about 5 %. Also in wetwell the formation of nitric acid is small and the pH of wetwell pool stays alkaline due to CsOH. In these results only the formation of nitric acid in water phases were calculated. This formation is very small and it is calculated that the dissolved nitrogen in water phase will be enough and do not limit this reaction.

References

Beahm e. V., et al. Iodine Evolution and pH control. NUREG/CR-5950, Oak Ridge National Laboratory. 1992.

E. Leppämäki, Pyrolysis Studies of Lipalon Cable, Organic Iodine Formation in Gas Phase, Technical Report F14S-CT96-0023, Appendix 1.

NRC, U. S. Nuclear Regulatory Commission, Regulatory Guide 1.25, Assumptions used for evaluating the potential radiological consequences of a fuel handling accident in the fuel handling and storage facility for boiling and pressurized water reactors. NRC 1972.

Murphy K.G. and K.M. Campe, "Nuclear Power Plant Control Room Ventilation System Design for Meeting General Design Criterion 19," in Proceedings of the 13th AEC Air Cleaning Conference, CONF-740807, U.S. Atomic Energy Commission, Washington, DC, 1974.

Weber C.F. Calculation of Absorbed Doses to Water Pools in Severe Accident Sequences. NUREG/CR-5808. Oak Ridge National Laboratory. 1991.

Eckerman K. F., Ryman J. C. 1993. External exposure to radionuclides in air, water and soil. Federal Guidance Report No. 12. EPA-402-R-93-081. Oak Ridge National Laboratory.

Kloosterman J.L. MARMER, A flexible point-kernel shielding code user manual version 2.0. Interfacultair Reactor Instituut. Delft, 1990.

ORIGEN 2.1 1991, Isotope Generation and Depletion Code, Matrix Exponential Method. RSIC Computer Code Collection CCC-371 (Revised August 1991).

Hack, K., Petersen, S., Koukkari, P. and Penttilä, K., "CHEMSHEET an Efficient Worksheet Tool for Thermodynamic Process Simulation", Microstructures, Mechanical Properties and Processes, Bréchet Y., Wiley (Ed.), EUROMAT, Vol. 3, 1999, pp 323-330.